

# Dyotropic Reactions: Mechanisms and Synthetic Applications<sup>†</sup>

Israel Fernández,<sup>\*,‡</sup> Fernando P. Cossío,<sup>§</sup> and Miguel A. Sierra<sup>‡</sup>

Departamento de Química Orgánica, Facultad de Química, Universidad Complutense, 28040-Madrid, Spain, and Kimika Organikoa I Saila—Departamento de Química Orgánica I, DIPC, Universidad del País Vasco—Euskal Herriko Unibertsitatea, P.K. 1072, 28080-San Sebastián Donostia, Spain

Received June 2, 2009

## Contents

1. Introduction	6687
2. Type I Dyotropic Rearrangements	6687
2.1. Thermal Reactions Involving Group 14–16 Elements as the Static Scaffold	6688
2.1.1. Group 14 Elements	6688
2.1.2. Group 15–16 Elements	6693
2.2. Thermal Reactions Involving Transition Metals	6694
2.3. Photochemical Reactions	6696
3. Type II Dyotropic Rearrangements	6696
3.1. Thermal Reactions	6696
3.2. Photochemical Reactions	6699
4. Theoretical and Computational Studies on Reaction Mechanisms	6699
4.1. Type I Dyotropic Processes	6699
4.1.1. Concerted Pathways	6699
4.1.2. Stepwise Mechanisms	6701
4.2. Type II Dyotropic Reactions	6703
4.2.1. Concerted Pathways: Synchronicity and Aromaticity	6704
4.2.2. Stepwise Pathways	6705
5. Applications of Dyotropic Rearrangements in Total Synthesis	6705
5.1. Synthesis of 23'-Deoxy Cephalostatin 1-Analogues	6705
5.2. Synthesis of the Proteasome Inhibitors TCM-95A and TCM-95B	6706
5.3. Applications of the Dyotropic Rearrangement of 5-Lithiodihydrofurans in Total Synthesis	6706
5.4. Synthesis of Azafenestrane	6707
6. Conclusions and Outlook	6708
7. Acknowledgments	6709
8. References	6709



Israel Fernández (Madrid, 1977) enjoyed studying chemistry at the Universidad Complutense of Madrid (UCM). In 2005, he earned his Ph.D. in Chemistry at the UCM under the supervision of Prof. Miguel A. Sierra and received the Prize for the best Doctoral Thesis in Synthetic Chemistry by the Spanish Royal Society of Chemistry and the Lilly-Young Researcher Prize. After that, he joined the Theoretical and Computational Chemistry group of Prof. G. Frenking at the Philipps Universität Marburg as a postdoctoral researcher studying the bonding situation and reaction mechanisms of organic and organometallic compounds. At the present, I.F. is a Ramón y Cajal fellow at the UCM. His current research includes the computational study of the bonding situation and reaction mechanisms of organic, organometallic, and bioorganic compounds with special interest in C–C bond forming processes.

without positional interchange (Scheme 1B,C). The uncatalyzed and concerted nature of these processes was also proposed.<sup>3,4</sup>

Nowadays, dyotropic transformations are standard tools for the construction of organic and organometallic molecules. Frequently, this unique rearrangement is the single entry to an efficient preparation of target molecules. Moreover, the discovery of new dyotropic reactions involving transition metals and excited states had widened the mechanistic scope of these processes to new reaction pathways well away from the original definition of uncatalyzed and concerted processes.

This review comprehensively reports the dyotropic reactions studied since the seventies, accounts for the different reaction mechanisms for these rearrangements, and discusses their synthetic applications in organic and organometallic chemistry.

## 2. Type I Dyotropic Rearrangements

Type I dyotropic rearrangements involve a 1,2-shift in which two migrating groups interchange their relative positions in a stationary scaffold (Scheme 1). The assumed *anti* conformation of the reactive scaffold forces the groups to migrate on opposite sides of the stationary framework,

## 1. Introduction

In 1972, M. T. Reetz defined dyotropic (from the greek *dyo*, meaning two) rearrangements as a new class of pericyclic valence isomerizations in which two  $\sigma$ -bonds simultaneously migrate intramolecularly.<sup>1,2</sup> Reactions in which the two migrating groups interchange their relative positions were designated as type I (Scheme 1A) whereas those of type II involve migration to new bonding sites

<sup>†</sup> This review is warmly dedicated to Prof. Gernot Frenking (Philipps-Universität Marburg).

\* To whom correspondence should be addressed. E-mail: israel@quim.ucm.es.

<sup>‡</sup> Universidad Complutense de Madrid.

<sup>§</sup> Universidad del País Vasco—Euskal Herriko Unibertsitatea and DIPC.



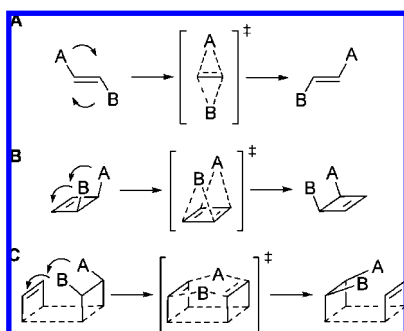
Fernando P. Cossio studied chemistry at the Universidad de Zaragoza (Spain) and received his Ph.D. in 1986 (Prof. C. Palomo). After a postdoctoral stay at CNRS (Talence, France, Dr. J.-P. Picard), he joined the University of the Basque Country (UPV/EHU) as Profesor Titular in 1988 and Catedrático in 2002. In 1994, after a short stay at UCLA in the laboratories of Prof. K. N. Houk, he decided to combine theoretical and experimental organic chemistry to investigate the origins of selectivity in chemical reactions. His research interests include pericyclic reactions (with special emphasis on thermal cycloadditions), C–C bond forming reactions, and medicinal chemistry.



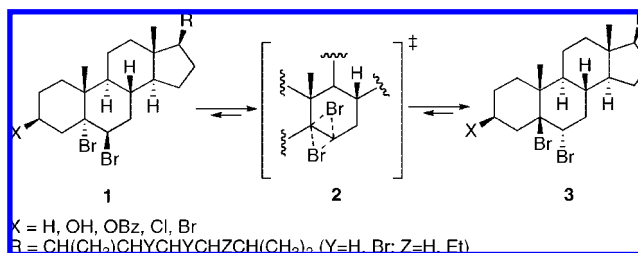
Miguel A. Sierra studied chemistry at the UCM (Madrid) and received his Ph.D. in 1987 (Honors). After a postdoctoral stay at Colorado State University (Prof. Louis Hegedus), he was promoted to Profesor Titular in 1990 and Catedrático in 2005 (UCM). His research encompasses the development of new processes based on transition-metal complexes, the study of organometallic reaction mechanisms, the preparation of new bioorganometallic compounds, and the design and synthesis of new energetic materials. He is the Secretariat of the Organic Chemistry Group of RSEQ and a Member of the Scientific Advisory Board of the Organization for the Prohibition of Chemical Weapons.

each suprafacially. This situation necessarily leads to inversion of the configuration at both atoms of the scaffold.<sup>3,4</sup>

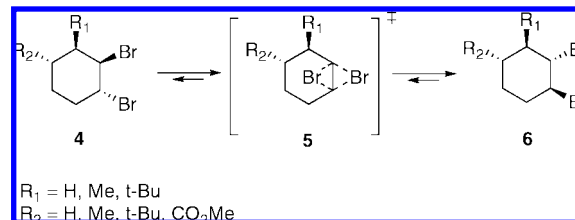
### Scheme 1. Type I (A) and Type II (B,C) Dyotropic Rearrangements



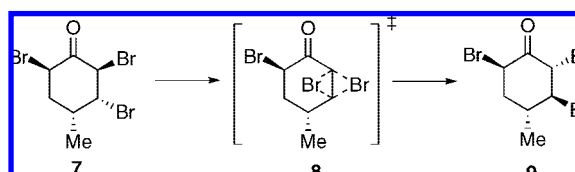
### Scheme 2



### Scheme 3



### Scheme 4



This section summarizes type I dyotropic rearrangements according to the nature of the atoms of the static scaffold (section 2.1), including processes which involve transition metals (section 2.2).

## 2.1. Thermal Reactions Involving Group 14–16 Elements as the Static Scaffold

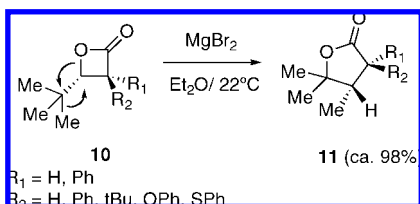
### 2.1.1. Group 14 Elements

**C–C Bond as Stationary Framework.** The mutarotation of vicinal dibromides in stereoidal systems, first studied by Grob and Winstein, was one of the earliest examples of a dyotropic rearrangement involving a C–C bond as the stationary scaffold.<sup>5</sup> Heating compounds **1** leads to the 1,2-migration of the bromine atoms with inversion of the configuration on both carbon atoms (Scheme 2). In the authors' words: "*It is considered probable that (...) an intermediate or transition state is involved with negligible charge separation, both bromine atoms being essentially equivalent*". The transition state nature of structures **2** in nonionizing solvents (heptanes) was subsequently suggested by Barton and Head.<sup>6</sup>

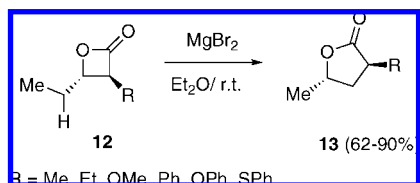
Berti and co-workers (Scheme 3)<sup>7</sup> and Grenier-Loustalot and co-workers (Scheme 4)<sup>8</sup> reported similar conclusions in the cyclohexanes **4** and cyclohexanones **7**, respectively. Recent computational work by us<sup>9</sup> and others<sup>10,11</sup> showed that these dyotropic reactions take place through highly synchronous symmetry-allowed mechanisms (*vide infra*). Both migrating bromine atoms are essentially equivalent in these complex asymmetric systems, matching the geometries postulated by Winstein<sup>5</sup> and Barton<sup>6</sup> in their pioneering works.

The transformation of 4-substituted- $\beta$ -lactones to butyrolactones is one of the most used types of I dyotropic reactions in organic synthesis. Mulzer and Brüntrup found that upon addition of  $\text{MgBr}_2$  to a THF-solution of **10**, a stereospecific

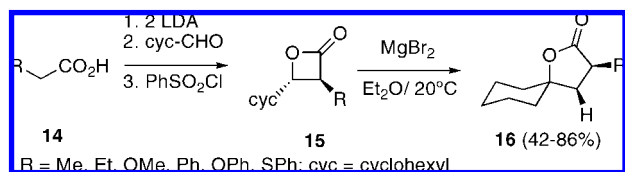
Scheme 5



Scheme 6



Scheme 7



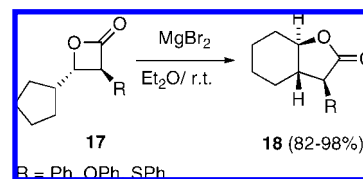
dyotropic rearrangement occurs at room temperature, producing butyrolactones **11** in excellent yields (Scheme 5).<sup>12</sup> This procedure allows the preparation of 3-substituted butyrolactones having substituents not available via the standard alkylation of the lactone enolates.<sup>13</sup> This process was formerly named as a Wagner–Meerwein type dyotropic rearrangement by analogy with the carbocation 1,2-rearrangements.<sup>14</sup>

Black and co-workers demonstrated the higher migratory aptitude of the hydrogen atom compared to alkyl groups in the above process.<sup>15</sup> No carbon migration was observed in the reactions depicted in Scheme 6. This experimental finding agrees with a conformation of **12** where the carbon–oxygen and carbon–hydrogen bonds are aligned in an *anti*-coplanar fashion (Scheme 6). The synthesis of 4,5-dihydro-5-methyl-3-(phenylthio)furan-2-(3H)-one (a key intermediate in the syntheses of both 6-angelicalactone<sup>16</sup> and ancephsenolide<sup>17</sup>) nicely reflects the synthetic power of this transformation.

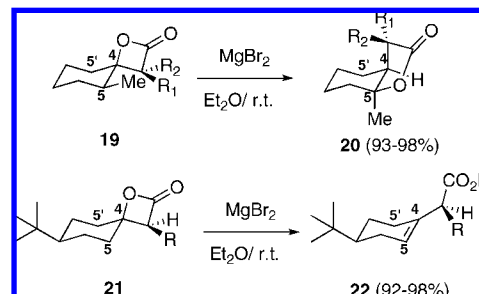
Black's group employed this procedure to prepare spiro-lactones **16** from cyclohexanecarboxyaldehyde and acid derivatives **14** (Scheme 7).<sup>18,19</sup> In principle, the three bonds to the cyclohexyl-carbon atom adjoining the lactone ring in **15** are capable of migration in the rearrangement step via simple rotation around the single bond joining the cyclohexane and lactone moieties. However, the essentially unrestricted rotation around the cyclohexyl–lactone bond favors the hydride migration due to the *trans*-relative relationship between the cyclohexane ring and the R-substituent. This result supports the requirement for a dyotropic rearrangement, namely that the migrating bonds should be capable of adopting a *trans* coplanar conformation to favor the maximum bond overlap in the corresponding transition state.<sup>4</sup>

This approach was used for the stereospecific construction of fused butyrolactones possessing three contiguous asymmetric centers.<sup>18,20</sup> Brief exposure of the  $\beta$ -lactone **17** to  $\text{MgBr}_2 \cdot \text{Et}_2\text{O}$  in  $\text{Et}_2\text{O}$  at room temperature formed the *trans,trans*-butyrolactone **18** (Scheme 8). It should be noted that the three contiguous asymmetric centers in compound

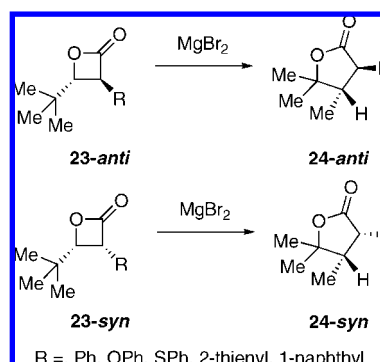
Scheme 8



Scheme 9



Scheme 10



**18** have the same relative configuration as different natural products (i.e.,  $\alpha$ -santonin and  $\alpha$ -artemisin).

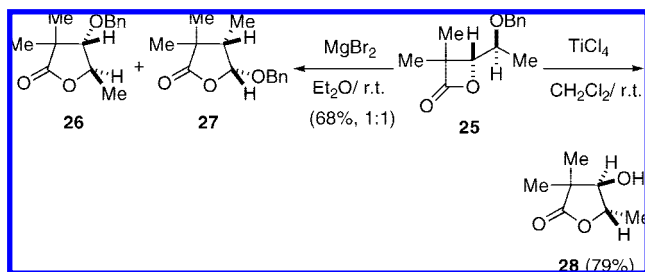
When the spiranic C4 has hydrogen atoms at both  $\alpha$ -carbons, instead of the expected ring enlargement due to a dyotropic transformation, a  $\beta$ -elimination reaction occurs. This fact was demonstrated in the reactions of  $\beta$ -lactones **19** and **21** with  $\text{MgBr}_2$  (Scheme 9).<sup>21–23</sup>

The stereospecificity of the type I dyotropic rearrangement was addressed by Black's group in the dyotropic rearrangements of *syn*- and *anti*- $\beta$ -lactones **23** to butyrolactones **24**. The *syn*- and *anti*-relative positions of lactones **23** and **24** are maintained during the simultaneous  $\sigma$ -bond migrations (Scheme 10),<sup>24</sup> which supports the concerted nature of these transformations.

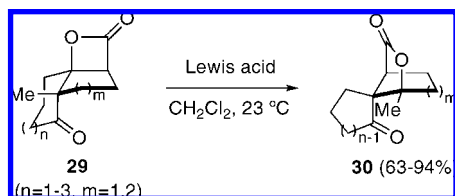
Interestingly, other Lewis acids such as  $\text{BF}_3$  or  $\text{Ti}(\text{O}^i\text{Pr})_4$  did not promote the rearrangement. In contrast, Cossío and co-workers reported that the behavior of the benzyloxy-substituted 2-oxetanones **25** is quite sensitive to the nature of the Lewis acid used to initiate the dyotropic rearrangement.<sup>25</sup> Thus,  $\text{MgBr}_2$  leads to the migration of both the benzyloxy and methyl groups, forming an equimolar mixture of products **26** and **27**, whereas  $\text{TiCl}_4$  only produces butyrolactone **28** (Scheme 11).

The dyotropic reactions involving a C–C bond as stationary scaffold recently reported by Romo and co-workers are related to the ring enlargement of  $\beta$ -lactones.<sup>26</sup> Thus, the addition of a Lewis acid to a  $\text{CH}_2\text{Cl}_2$  solution of  $\beta$ -lactones **29**, which possess the required antiperiplanar relationship between the migrating C–O bond of the  $\beta$ -lactone and the

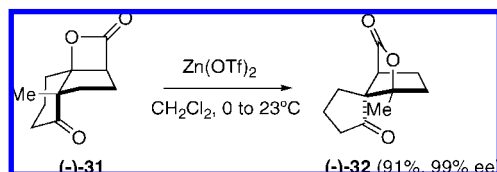
Scheme 11



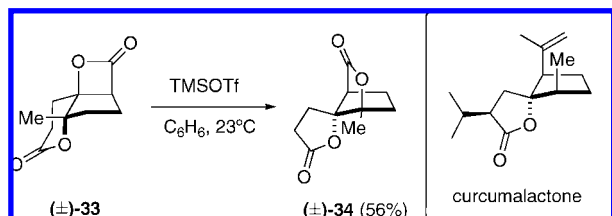
Scheme 12



Scheme 13



Scheme 14

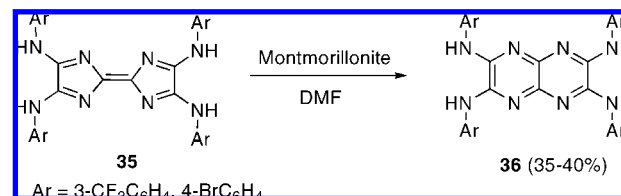


$\text{C}-\text{C}=\text{O}$  bond, provokes the expected ring expansion, leading to the spiro- $\gamma$ -lactone **30** at room temperature (Scheme 12). Among the Lewis acids employed, the best results were found using  $\text{E}(\text{OTf})_3$  ( $\text{E} = \text{Yb}$  and  $\text{In}$ ) and  $\text{ZnX}_2$  ( $\text{X} = \text{Cl}$ ,  $\text{Br}$ ,  $\text{OTf}$ ). The use of  $\text{Mg}(\text{II})$  salts ( $\text{MgBr}_2 \cdot \text{Et}_2\text{O}$  or  $\text{Mg}(\text{OTf})_2$ ) fails to promote this process. The asymmetric variant of this reaction has also been reported in the conversion of  $(-)$ -**31** to  $(-)$ -**32**. This transformation occurs in excellent yield and with high stereochemical fidelity (99% ee, Scheme 13). It has been suggested that the rearrangement occurs concertedly through an 1,2-acyl migration via the corresponding four-membered transition state.

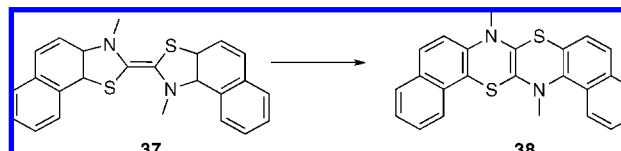
Using the same methodology, spiro-lactone **34** (the core of the natural product curcupalactone) is formed through a 1,2- $\delta$ -lactone dyotropic rearrangement from bis-lactone **33** (Scheme 14).<sup>26</sup>

The transformation of tetraazafulvalenes **35** to the strongly fluorescent 1,4,5,8-tetraazanaphthalenes **36** in the presence of montmorillonite-clay occurs by a type I dyotropic rearrangement (Scheme 15).<sup>27</sup> It has been suggested that the inclusion of the extended  $\pi$ -electron system of **35** facilitates this symmetry forbidden  $[\sigma_2 + \sigma_2]$ -process. These results allow the interpretation of earlier reactions reported for analogous heterofulvalenes (Scheme 16)<sup>28</sup> and fulvenes (Scheme 17)<sup>29</sup> as dyotropic rearrangements. The rearrangement of **35** in the presence of K10 and DMF is an easy entry to otherwise hardly accessible ring-fused pyrazines of type **36**.

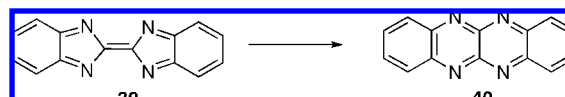
Scheme 15



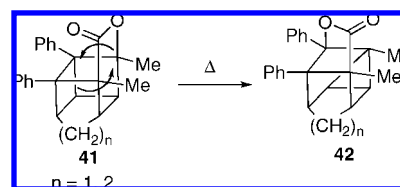
Scheme 16



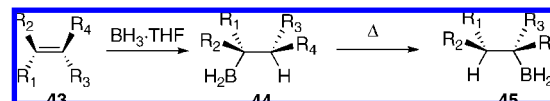
Scheme 17



Scheme 18



Scheme 19



A  $[\sigma_2 + \sigma_2]$  1,2-dyotropic reaction has also been found in compressed cage compounds. In fact, when a benzene solution of  $\delta$ -lactone **41** is passed through a preheated quartz column at  $350^\circ\text{C}$ , formation of isomer **42** is observed (Scheme 18).<sup>30</sup> The mechanistic studies indicate first-order kinetics with activation barriers ranging from 29 to 36 kcal/mol and  $\Delta S^\ddagger$  in the range of  $-20$  to  $-6$  eu, which is in the line of other type I dyotropic processes.<sup>4</sup> Despite the fact that thermal  $[\sigma_2 + \sigma_2]$  reactions are usually symmetrically forbidden processes, these reactions may become thermally allowed process due to the participation of the lone pair of the oxygen atom (vide infra).

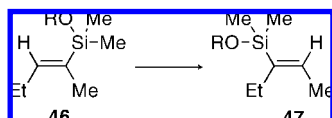
Knochel and co-workers reported the 1,2-migration depicted in Scheme 19. The sterically hindered organoboranes **44** thermally undergo a stereoselective 1,2-*syn*-dyotropic migration (Scheme 19).<sup>31</sup> Albeit predictable, the stereoselectivity of the migration strongly depends on the structure of the initial alkene and on the reaction conditions. It should be noted that this is an example of a type I *syn*-dyotropic rearrangement.

The isomerization of 2-silyloxy-substituted pentenes **46** to 3-silyloxy-pentenes **47** (Scheme 20)<sup>32</sup> is the single additional case of type I *syn*-dyotropic rearrangement. The change from a type I *anti*-dyotropic rearrangement to a type I *syn*-dyotropic rearrangement may point to a nonconcerted mechanism as responsible for the observed reaction products.

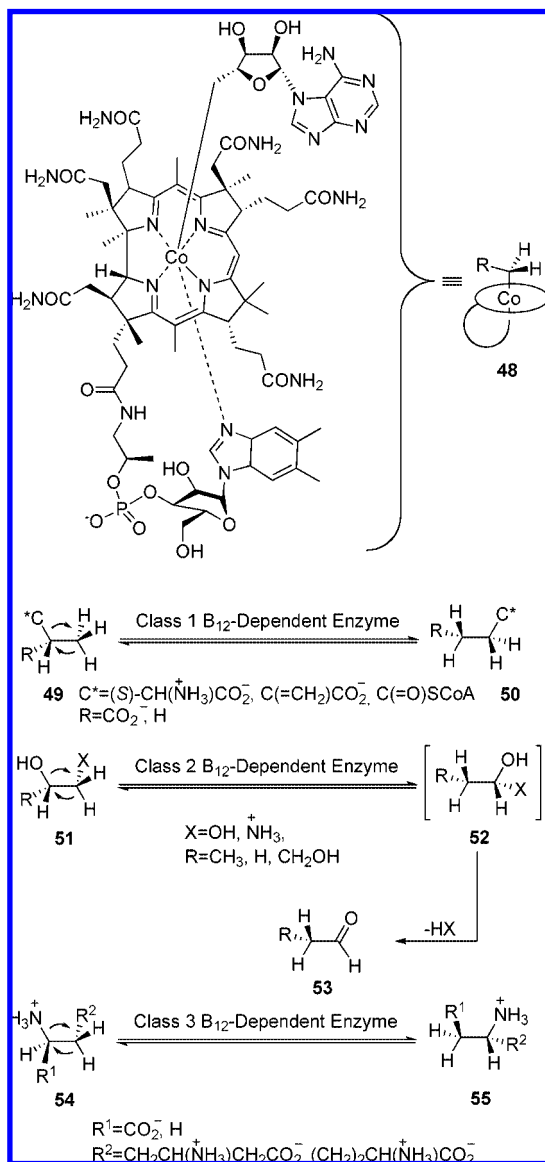
Dyotropic rearrangements are also catalyzed in biological systems by a family of isomerases that use adenosyl



Scheme 20

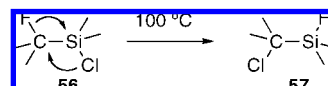


Scheme 21

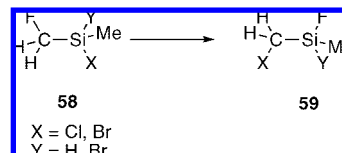


cobalamin (coenzyme B<sub>12</sub>) as a cofactor (Scheme 21). In these reactions, a Y group and an hydrogen atom interchange positions with inversion of configuration at the two static carbon atoms. The corresponding rearranged products play important roles in many metabolic pathways.<sup>33</sup> Class 1 B<sub>12</sub>-dependent isomerases catalyze transformations in which the Y group contains a carbon atom (Scheme 21). The most important members of this group are glutamate mutase,<sup>34</sup> 2-methyl glutarate mutase,<sup>35</sup> methyl malonyl-coenzyme A mutase,<sup>36</sup> and isobutyryl-coenzyme A mutase.<sup>37</sup> In class 2 B<sub>12</sub>-dependent isomerases, the migrating moieties Y can be amino or hydroxy groups and the resulting products are hydrates or geminal amino alcohols **52** that yield the corresponding carbonyl compounds **53** (Scheme 21). The best known members of this family of isomerases involved in dyotropic rearrangements are diol dehydratase,<sup>38</sup> glycerol dehydratase,<sup>39</sup> and ethanolamine-ammonia lyase.<sup>40</sup> Finally,

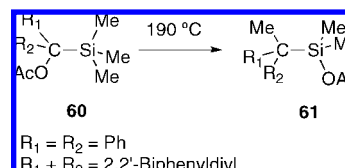
Scheme 22



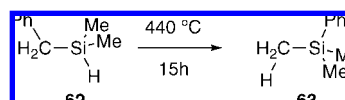
Scheme 23



Scheme 24



Scheme 25



in class 3 B<sub>12</sub>-dependent isomerases, Y stands for migrating amino groups of amino acids that are activated by pyridoxal phosphate. The most representative examples of these isomerases are L-β-lysine-5,6-aminomutase,<sup>41</sup> L-β-lysine-2,3-aminomutase,<sup>42</sup> and D-ornithine 4,5-aminomutase.<sup>43</sup>

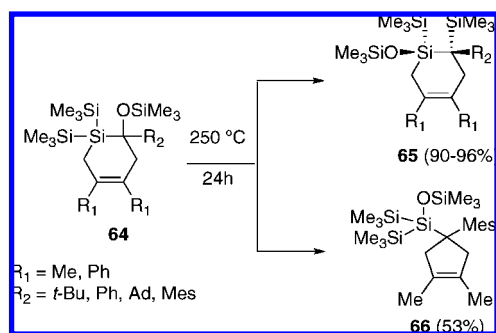
**Silicon to Tin in the Static Scaffold.** Several type I dyotropic reactions involving the heavier analogues of carbon (mainly silicon) have been studied. The C–Si analogue of dihalide migration in cyclohexanes and cholestanes (Schemes 2 and 3) has been reported by Hazeldine and co-workers (Scheme 22).<sup>44</sup> This transformation, which exhibits a first-order kinetics, uses a C–Si bond as static scaffold and requires comparable temperatures to those needed for the analogous rearrangement with C–C bonds as the static scaffold. Similar processes involving phenyl groups and such nucleofugal moieties as fluorine, chlorine, and acetate moieties were reported earlier by Brook.<sup>45</sup>

Bürger and Moritz observed a similar 1,2-dihalide migration during the preparation of (fluoromethyl)silicon derivatives from (fluorodibromomethyl)silane precursors.<sup>46</sup> Thus, compounds **59** were quantitatively obtained from **58** through a dyotropic rearrangement (Scheme 23). In all cases and as expected for this rearrangement, inversion of configuration on both carbon and silicon atoms is observed.

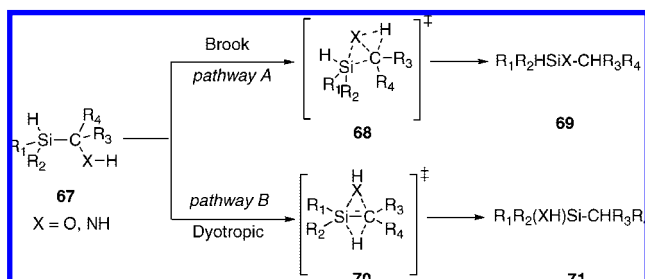
The thermal quantitative exchange of acetate and methyl groups in **60** is closely related to the above transformations (Scheme 24).<sup>47</sup> Mechanistic studies indicate first-order kinetics with activation barriers of ca. 34 kcal/mol and ΔS<sup>‡</sup> ca. –6 eu. These values and the independence of the velocity of the reaction with the polarity of the solvent are fully consistent with related type I dyotropic processes.<sup>4</sup> The phenyl–hydrogen exchange depicted in Scheme 25 requires more drastic reaction conditions.<sup>48</sup> The studies reported by Claes and Deleuze<sup>49</sup> show significant entropic contributions to the activation energies of these thermal rearrangements upon increasing reaction temperatures. These data point to dissociative pathways involving silyl radicals.

Heating of silacyclohexenes **64** in a degassed sealed tube at 250 °C for 24 h results in a clean reaction to give the

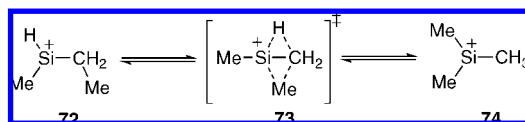
Scheme 26



Scheme 27



Scheme 28



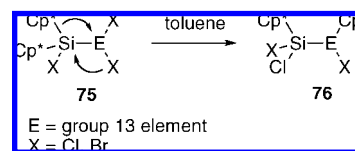
*cis*-silacyclohexenes **65** in excellent yields (Scheme 26).<sup>50</sup> The corresponding *trans*-isomer is not detected in these reactions, thus confirming the stereoselectivity of the transformation. Furthermore, when  $\text{R}^1 = \text{Me}$  and  $\text{R}^2 = \text{Mes}$  (see Scheme 26), cyclopentene **66** was obtained. This example shows that the dyotropic rearrangement can involve one endocyclic methylene and the trimethylsilyloxy group instead of one trimethylsilyl group and one trimethylsilyloxy group.

Silanes **67** lead to the formation of compounds **69** and/or **71** (Scheme 27).<sup>51–53</sup> Two main reaction pathways have been explored for these transformations: the Brook rearrangement<sup>54</sup> (pathway A) and the 1,2-dyotropic process (pathway B). Experimental and computational (*vide infra*) studies indicate that the dyotropic process is both thermodynamically and kinetically favored, with the Brook rearrangement being competitive only at high temperatures.

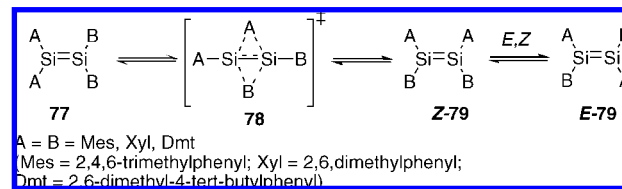
Hydrogen–chlorine<sup>55</sup> or hydrogen–methyl<sup>56</sup> exchanges on a C–Si single bond have also been reported in the gas phase. Experiments with labeled reagents suggest that  $\text{Si}(\text{CH}_3)_3^+$  (**74**) and  $\text{HSi}(\text{CH}_3)(\text{C}_2\text{H}_5)^+$  (**72**) cations interconvert by multiple low-energy collisions through a dyotropic rearrangement via the corresponding cyclic transition state **73** (Scheme 28). Fragmentation to  $\text{H}_2\text{Si}(\text{CH}_3)^+$  and  $\text{C}_2\text{H}_4$  competes with the isomerization, suggesting that the isomerization barrier is similar in energy to the fragmentation barrier. In contrast, using the same multiple low-energy collision method, it was found that  $\text{H}_2\text{Si}(\text{C}_2\text{H}_5)^+$  and  $\text{HSi}(\text{CH}_3)_2^+$  can be induced to interconvert without competing fragmentation. These results were later revisited by Graul and Willard,<sup>57</sup> who found a lower energy reaction pathway for both interconversions, and therefore, the proposed dyotropic mechanisms were discarded.

Type I dyotropic rearrangements involving silicon atoms are not restricted to C–Si bonds. Jutzi and co-workers

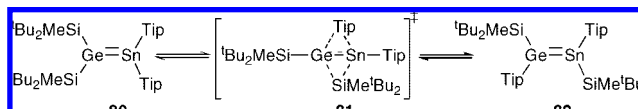
Scheme 29



Scheme 30



Scheme 31

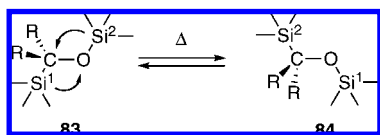


proposed a dyotropic transformation in the reaction of decamethylsilicocene with group 13 halides.<sup>58</sup> Thus, pentamethylcyclopentadiene ( $\text{Cp}^*$ ) and the halide interchange their relative positions on the static Si–E (E = group 13 element) bond (Scheme 29). According to the initial suggestion by Reetz,<sup>3,4</sup> the presence of the  $\pi$ -system of the  $\text{Cp}^*$  ligand facilitates the process, since it can easily interact with and migrate to a neighboring element center.

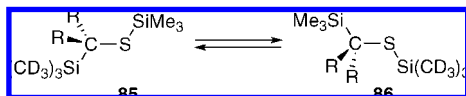
1,2-Dyotropic rearrangements have also been proposed within a Si=Si double bond. Compounds **77** experience a stereoselective and intramolecular exchange of two aryl substituents between the silicon atoms to produce compounds *E,Z*-**79** (Scheme 30).<sup>59</sup> When A = Mes and B = Xyl, the rearrangement is found to be first order with  $\Delta H^\ddagger = 15.2$  kcal/mol and  $\Delta S^\ddagger = -36.4$  eu, which is in nice agreement with a concerted dyotropic mechanism proceeding through a bicyclic transition state (nevertheless, an alternative stepwise mechanism involving disilene–silylsilylene rearrangement may not be safely excluded). In clear contrast, similar processes for the analogous tetraarylethenes have not been reported to date. These differences occur because the Si=Si double bond on compounds **77** is twisted with a planar arrangement around each of the unsaturated silicon atoms.<sup>60</sup> The twisted Si=Si bond facilitates the dyotropic rearrangement in silenes compared to the analogous ethenes.

The heavier elements of group 14 undergo a similar process. Sekiguchi and co-workers found that the asymmetrically substituted germa-stannaene **80**, a stable compound at room temperature, easily and quantitatively isomerizes upon heating to form the corresponding symmetrically substituted isomer (*E*)-1,2-bis(di-*tert*-butylmethylsilyl)-1,2-bis(2,4,6-triisopropylphenyl)-1-germa-2-stannaene (**82**) (Scheme 31).<sup>61</sup> Such an isomerization may proceed by the simultaneous dyotropic 1,2-shifts of silyl and aryl groups from Ge to Sn and from Sn to Ge atoms, respectively, through the initial twisting of the Ge=Sn double bond, followed by a bicyclobutane-type transition state to form the more stable *E* isomer **82**. This mechanistic proposal was made on the basis of the experimental activation parameters [ $\Delta H^\ddagger = 22$  kcal/mol and  $\Delta S^\ddagger = -12$  cal/(K mol)], which are consistent with a concerted reaction pathway via a rigid transition state **81**.

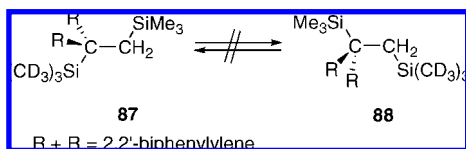
Scheme 32



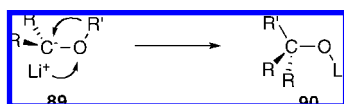
Scheme 33



Scheme 34



Scheme 35



### 2.1.2. Group 15–16 Elements

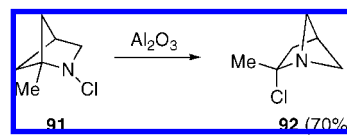
Most of the type I dyotropic reactions, which involve a C–O bond as static scaffold, were studied by the Reetz's group and have already been summarized in his review of 1977.<sup>4</sup> Therefore, only the most representative processes are summarized, especially those related to further mechanistic proposals.

The type I dyotropic exchange in a C–O bond as static scaffold has been studied using compounds **83** (Scheme 32).<sup>62</sup> Aryl groups were chosen as the substituents attached to the carbon atom both to avoid undesired side reactions, such as silanol elimination, and to facilitate the rearrangement. The mechanistic studies, which include deuteration experiments, indicate that the reaction is intramolecular with an activation barrier of ca. 31 kcal/mol and negative activation entropy [ca.  $\Delta S^\ddagger = -9$  cal/(K mol)]. Moreover, the reaction rate is not influenced by the polarity of the reaction solvent while the presence of  $\pi$ -donor substituents in the aryl groups slows the transformation. Retention of configuration is observed in the migrating silyl groups whereas inversion is found at the stationary carbon atom. Therefore, all data point to a concerted reaction pathway through the corresponding bicyclic transition state.<sup>4,63</sup>

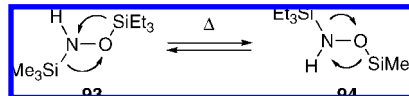
The similar transformation using the thioether **85** was also studied (Scheme 33).<sup>64</sup> This reaction requires more drastic conditions (>10 h at 230 °C) to produce only 10% of the rearranged product **86**. Compound **85** rearranges 4 orders of magnitude more slowly than the oxygen analogue **83**, which is very likely due to the vastly different Si–X bond strengths ( $E_{\text{Si-O}} - E_{\text{Si-S}} \approx 30$  kcal/mol).<sup>65</sup> The corresponding compound **87**, where the heteroatom of **85** was replaced by a carbon atom, did not rearrange (Scheme 34).

The Wittig rearrangement is usually classified as a sigmatropic shift in which an alkyl group migrates from oxygen to the neighboring lithiated carbon atom.<sup>66</sup> However, should the counterion be included in the process,<sup>67</sup> a dyotropic transformation will evolve (Scheme 35). Thus, Wittig rearrangement may be interpreted as a type I dyotropic rearrangement in which R migrates from oxygen to carbon

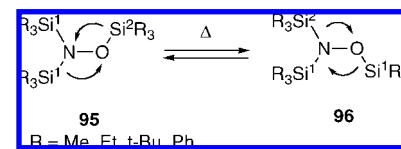
Scheme 36



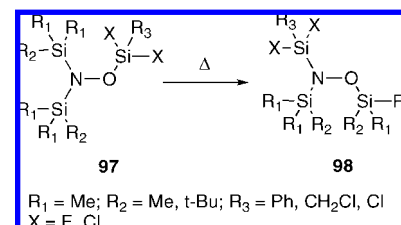
Scheme 37



Scheme 38



Scheme 39



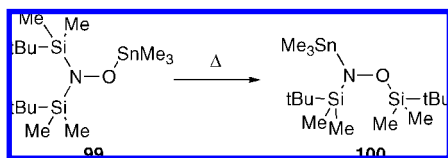
with retention of the configuration while lithium migrates from carbon to oxygen with “inversion”.<sup>4</sup>

Type I 1,2-dyotropic rearrangements involving a C–N bond as stationary scaffold are rare. The single example known was described by Malpass and co-workers in 1985.<sup>68</sup> Upon addition of alumina to a solution of L-methyl-2-chloro-2-azabicyclo[2.1.1]hexane **91**, a rearrangement occurs to produce the derivative **92** in 30 min with a 70% yield (Scheme 36). The transformation may be either viewed formally as a dyotropic shift or, alternatively, as producing an intimate ion pair in which the buildup of positive charge is, predictably, at carbon atom rather than at nitrogen atom.

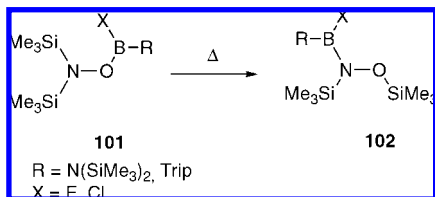
In contrast, numerous type I dyotropic processes have been found in the rearrangements of hydroxylamines, therefore involving O–N bonds as the static framework. Frainnet and co-workers<sup>69</sup> described this transformation in derivative **93** (Scheme 37). No symmetric products were observed, which points to an intramolecular transfer of the silyl moieties. Systematic studies on the rearrangements of tris(silyl)hydroxylamines **95** have been reported by West's group (Scheme 38).<sup>70</sup> Thermolysis of compounds **95** reveals that the intramolecular rearrangement is reversible and general, but it is hampered by steric hindrance due to bulky substituents at silicon atom. In fact, increased steric bulk at silicon seems to decrease the ability to reach the optimal geometry for a double migration. The reaction rates are unaffected by changes in the concentration or solvent polarity with activation parameters quite similar to those for other related dyotropic transformations [ $\Delta H^\ddagger = 30$  to 38 kcal/mol and  $\Delta S^\ddagger = -3$  to  $-11$  cal/(K mol)].

Similarly, Klingebiel and co-workers studied the analogous rearrangement using halogen (F, Cl) substituted silyl groups attached to the oxygen atom in compounds **97** (Scheme 39).<sup>71–73</sup> This group has reported a similar process involving a silyl–stannyl exchange (Scheme 40).<sup>71</sup> No significant

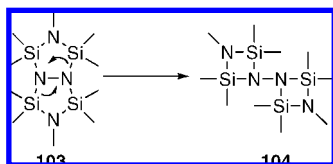
Scheme 40



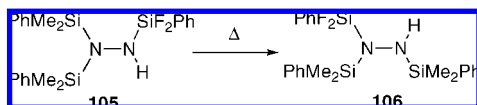
Scheme 41



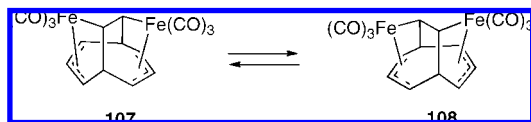
Scheme 42



Scheme 43



Scheme 44



differences with respect to the silyl–silyl exchange were found (vide infra). A boron–silicon migration is also feasible in hydroxylamines **101** (Scheme 41).<sup>74</sup>

Hydrazines undergo a similar 1,2-silyl dyotropic rearrangement. Wannagat invoked a silyl–silyl valence isomerization to explain certain transformations in silylated hydrazines **103** (Scheme 42).<sup>75</sup> More recently, it has been reported that silylhydrazine **105** is transformed in **106** upon heating in THF. This result shows that a N–N bond can also serve as static scaffold for dyotropic processes (Scheme 43).<sup>76</sup> The computed activation barrier (ca. 37 kcal/mol) for the latter reaction is similar to that found for 1,2-silyl migrations in the parent silyl-hydroxylamines.

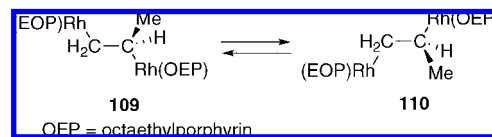
## 2.2. Thermal Reactions Involving Transition Metals

1,2-Dyotropic rearrangements may involve transition metals either as the stationary scaffold or as the migrating fragments.

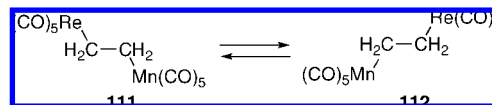
### Migrating Transition Metals in Type I 1,2-Dyotropic Rearrangements

Several examples of metal moieties acting as migrating fragments in type I 1,2-dyotropic rearrangements within a C–C stationary framework have been reported. Aumann described the 1,2-migration of the Fe(CO)<sub>3</sub> fragment in the isomerization of complex **107** (Scheme 44).<sup>77</sup> Similarly, a facile stereospecific 1,2-exchange of Rh(OEP) groups (OEP

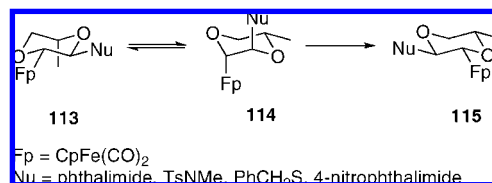
Scheme 45



Scheme 46



Scheme 47



= octaethylporphyrin) has been observed in complex **109** (Scheme 45).<sup>78</sup> Despite the fact that the activation parameters [ $\Delta H^\ddagger = 12.4 \pm 0.5$  kcal/mol and  $\Delta S^\ddagger = -10.7 \pm 1.9$  cal/(K mol)] for the conversion of **109** to **110**, determined by NMR line-shape analysis, are in agreement with those reported for other dyotropic processes, the possibility of the reaction occurring through a stepwise mechanism cannot be safely discarded.

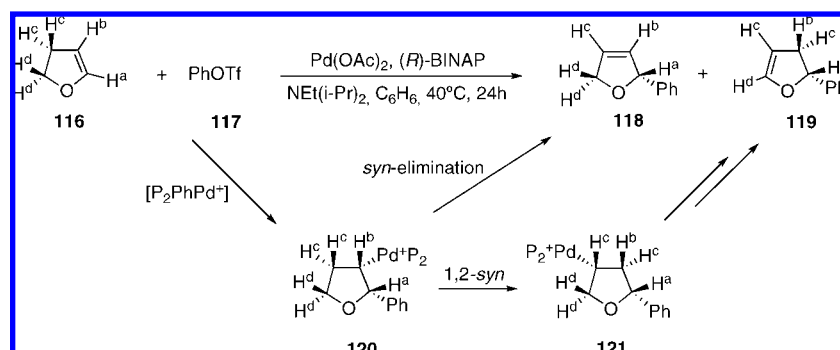
The dynamic behavior of complex **111** in solution has been rationalized through a 1,2-type I dyotropic shift (Scheme 46).<sup>79</sup> Similarly, complexes **113** rearrange in THF solution to their isomers **114** by simultaneous migration of the Nu and CpFe(CO)<sub>2</sub> groups (Scheme 47).<sup>80</sup> This process is closely related to the 1,2-dihalide exchange in cyclohexanes.<sup>7,8</sup> The dyotropic rearrangement in enantiomerically pure organoiron complexes **113** occurs with inversion at the two adjacent carbon centers. Again, kinetic studies show that this process follows first-order kinetics with activation parameters of  $\Delta H^\ddagger = 19.4$  kcal/mol and  $\Delta S^\ddagger = -12.9$  cal/(K mol) at 25 °C, which nicely supports an intramolecular concerted reaction mechanism.

An unusual type I *syn*-1,2-dyotropic shift has been proposed to explain the reaction products distribution of the asymmetric Heck reaction between phenyl triflate and various deuterated 2,3-dihydrofurans **116** (Scheme 48).<sup>81</sup> No evidence to support the usual *anti*-1,2-dyotropic shifts or *anti*- $\beta$ -H Pd eliminations during the formation of **118** and **119** was observed. Nevertheless, whether these *syn*-rearrangements occur via type I *syn*-1,2-dyotropic shifts or through a *syn*-“chain-walking” mechanism remains unclear.

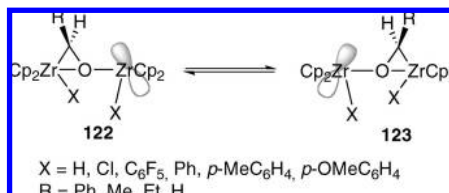
Erker and co-workers have studied the fluxional behavior of binuclear zirconocene complexes **122** in solution.<sup>82,83</sup> Using dynamic NMR spectroscopy, the degenerate rearrangement of **122** to **123** can be studied by using unsymmetrical bridging  $\mu$ -aldehyde ligands (Scheme 49). The observed thermally induced isomerization of complexes **122** proceeds through a concerted intramolecular exchange of Cp<sub>2</sub>ZrX units relative to the pivotal  $\mu$ -aldehyde ligand bridging both transition-metal centers. Strikingly, the activation barrier of the process is in the range of around 20 kcal/mol (when X = H; R = Me, Ph) to 7 kcal/mol (when X = Cl; R = H). This contrasts with the analogous process involving a silyl exchange, which requires temperatures



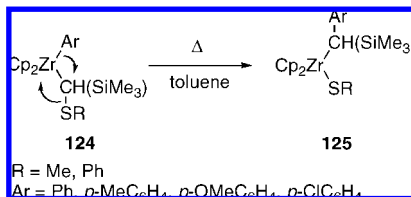
Scheme 48



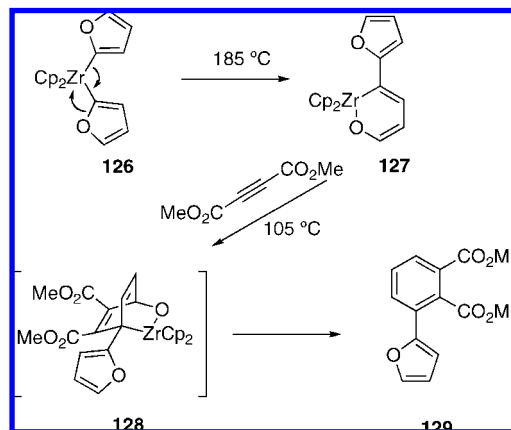
Scheme 49



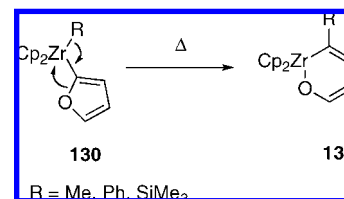
Scheme 50



Scheme 51



Scheme 52



above  $170^\circ\text{C}$ . The surprisingly low activation barriers for the isomerization of complexes **122** may be the result of the already formed metal–oxygen bond in the ground state. The consequence is that the ground state of complexes **122** is structurally much more akin to the transition state of the dyotropic rearrangement than the one for the silicon compounds **56** (see Scheme 22). Additionally, the migration of the second metal atom in **122** is favored by the presence of an acceptor orbital which is ideally located to interact with the carbon center of the pivot (Scheme 49).<sup>84</sup> Analogous rearrangements have also been observed in isostructural Hf–Hf and Zr–Hf dinuclear complexes having  $\mu$ -benzophenone bridging ligands,<sup>85</sup> in dinuclear zirconium hydride complexes having fulvene as a ligand,<sup>86</sup> and in the corresponding mononuclear complexes where a zirconocene unit was replaced by a  $\text{OSiR}_3$  ( $\text{R} = \text{Me}, \text{Et}, \text{iPr}, \text{Ph}$ ) group.<sup>87</sup> These results clearly show that the type I 1,2-dyotropic rearrangement is a general feature of this kind of organometallic complexes.

### Transition Metals in the Static Scaffold of Type I 1,2-Dyotropic Rearrangements

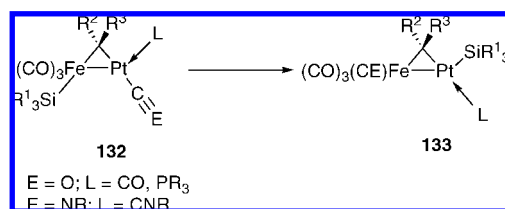
Type I thermal dyotropic reactions in substrates having a transition metal in the stationary framework are rare. Mintz and co-workers reported the thermal 1,2-dyotropic rearrangement of  $\alpha$ -zirconocenyl thioethers **124**, leading to the irreversible formation of complexes **125** (Scheme 50). The transformation follows first-order kinetics, and labeling experiments clearly showed that the rearrangement is intramolecular. The activation parameters were found to be in the usual range of type I dyotropic reactions [ $\Delta H^\ddagger = \text{ca. } 20 \text{ kcal/mol}$  and  $\Delta S^\ddagger = \text{ca. } -19 \text{ cal/(K mol)}$ ]. Methyl or benzyl

instead of aryl substituted complexes **124** fail to experience the above isomerization, probably due to the lower migratory aptitude of these groups in related nucleophilic migrations.<sup>88</sup>

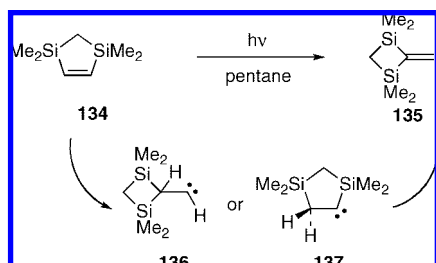
Erker's group has described a closely related dyotropic transformation which also involves the zirconocene moiety. Thus, bis(2-furyl)zirconocene cleanly undergoes a 1,2-dyotropic rearrangement at  $185^\circ\text{C}$  to yield the metallacyclic oxazirconacyclohexadiene derivative **127** (Scheme 51).<sup>89</sup> Complex **127** reacts with dimethyl acetylenedicarboxylate in a Diels–Alder/retro-Diels–Alder sequence to produce  $(\text{Cp}_2\text{ZrO})_3$  and dimethyl 3-(2-furyl)phthalate (**129**). This methodology was used to thermally induce ring enlargements, thus forming novel metallacycles.<sup>90</sup> Complexes **130**, where one of the two furyl groups of complex **126** is replaced by a Me, Ph, or a  $\text{SiR}_3$  group, also undergo a 1,2-type I dyotropic rearrangement to produce the cyclic complexes **131** (Scheme 52). Strikingly, the analogous bis(2-thienyl)zirconocene complex decomposes at  $185\text{--}200^\circ\text{C}$  to give  $[\text{Cp}_2\text{ZrS}]_2$  as the major organometallic product.

Braunstein and co-workers recently reported a type I 1,2-dyotropic rearrangement involving a Fe–Pt bond.<sup>91</sup> Triangular complexes **132** evolve to complexes **133** through the migration of the silyl group from iron to platinum with the concomitant 1,2 migration of CO from Pt to Fe (Scheme 53). Computational studies carried out on model compounds

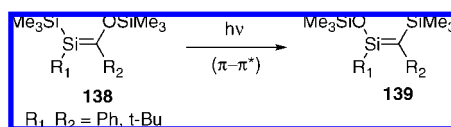
Scheme 53



Scheme 54



Scheme 55



indicate that the corresponding transition state of the transformation exhibits a triply bridged intermetallic bond (which is expected for a concerted dyotropic rearrangement).<sup>92</sup> Moreover, the low computed activated barrier (vide infra) shows that the isomerization process can be achieved at room temperature, which agrees with the experimental findings.

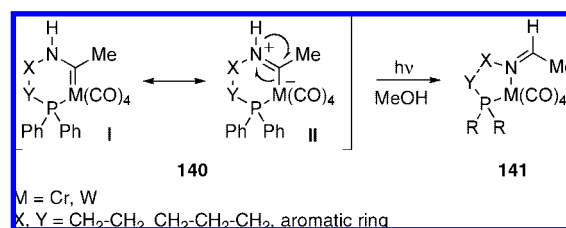
### 2.3. Photochemical Reactions

Type I 1,2-dyotropic rearrangements may also be promoted photochemically. Either concerted or stepwise reaction pathways in the excited state have been proposed for these processes.

Direct photolysis of disilacyclopentene **134** in pentane at 185–254 nm leads to the formation of 1,1,3,3-tetramethyl-2-methylene-1,3-disilacyclobutane **135**. A type I 1,2-dyotropic rearrangement in the excited state has been suggested to explain these results (Scheme 54).<sup>93</sup> According to this proposal, the transformation of **134** to **135** proceeds stepwise via the formation of the carbene **136** (through initial migration of the silyl group) and subsequent 1,2-shift of the hydrogen atom. However, no clear evidence has been found to unambiguously discard the alternative route involving the initial migration of the hydrogen atom to form the carbene **137** followed by 1,2-shift of the silyl group.

Closely related to the above process, the photoisomerization of silene **138** to **139** may also occur via a dyotropic transformation (Scheme 55).<sup>94</sup> Thus, the excitation of **138** leads to an excited twisted state of this sterically crowded molecule, which may be reasonably stable and long-lived. The twisted geometry of this excited state (either as a singlet or triplet), and its orbitals, appear appropriate to facilitate the required siloxy and silyl shifts (by a 1,2-dyotropic rearrangement), ultimately giving the rearranged silene **139**, presumably in its ground state. The invoked twisted geometry strongly resembles that found in the thermal 1,2-dyotropic isomerizations within Si=Si double bonds.<sup>59</sup>

Scheme 56



Photochemical type I 1,2-dyotropic rearrangements involving transition metals have also been reported. Irradiation of aminophosphino-chromium(0) carbene complexes **140** in the presence of MeOH yield new organometallic complexes **141** lacking the carbene moiety (Scheme 56).<sup>95</sup> This transformation is formally a type I 1,2-dyotropic rearrangement where both C–Cr and N–H bonds migrate intramolecularly; the Cr and H atoms interchange their relative positions, with the C=N moiety (structure II contributes significantly to the description of the complex) being the static scaffold (Scheme 56).

Quantum chemical calculations show that the reaction does not occur concertedly. Instead, a stepwise mechanism that starts with a short-lived triplet state, formed after initial photoexcitation of the singlet ground state  $S_0$  to the excited singlet state  $S_1$  and subsequent intersystem crossing, was found (vide infra). This dyotropic reaction is not restricted to chromium(0) carbene complexes. In fact, the corresponding isostructural aminotungsten(0) carbene complexes also form *syn-N*-metalated imines.<sup>96</sup> This process represents the very first photoreaction reported for Fischer type tungsten(0) carbene complexes, which have been traditionally considered as photoinert compounds. Computations indicate that tungsten(0) carbene complexes follow a similar reaction mechanism with no systematic differences between isostructural chromium(0) and tungsten(0) complexes.<sup>97</sup>

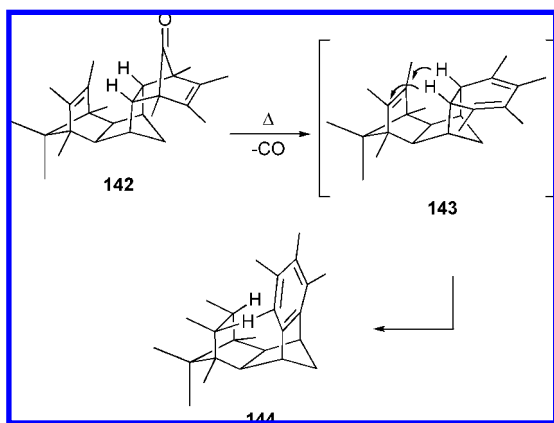
### 3. Type II Dyotropic Rearrangements

As stated above, those reactions in which the two migrating groups do not interchange their relative positions but are placed in new bonding sites are designated as type II dyotropic rearrangements. Thermally and photochemically promoted examples of such processes shall be described in sections 3.1 and 3.2, respectively.

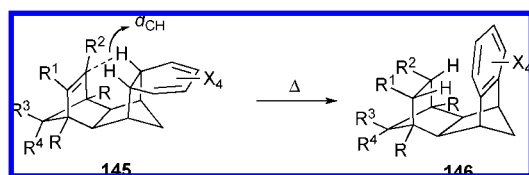
#### 3.1. Thermal Reactions

Reported type II dyotropic shifts mostly involve a double hydrogen migration in a carbon skeleton. These transhydrogenation reactions constitute a special class of the denominated double group transfer reactions as defined originally by Woodward and Hoffmann.<sup>98</sup> In 1965 the thermal [ $\sigma_2s + \sigma_2s + \pi_2s$ ] rearrangement leading from **143** to **144** (Scheme 57) was initially described as a sigmatropic hydrogen transfer in the isodrin series.<sup>99–101</sup> This initial finding was further extended to similar alicyclic frameworks containing a cyclohexa-1,3-diene or a 2-pyrazoline moiety (Schemes 58 and 59).<sup>102–104</sup> Both *syn*-sesquiorbonene derivatives **145** and **147** experience irreversible and exothermic type II dyotropic shifts promoted by the aromatization of the diene ring and the release of the ring-strain at the receptor  $\pi$ -bond. Although pyrazolines **147** are less reactive than trienes **145**, both compounds show similar reaction rates. Interestingly, chlorine or alkoxy substitution of the  $\pi$ -acceptor

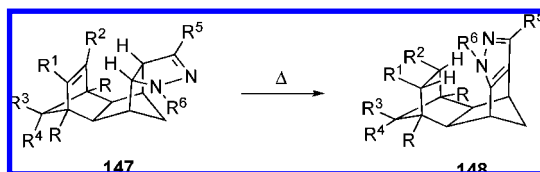
Scheme 57



Scheme 58



Scheme 59

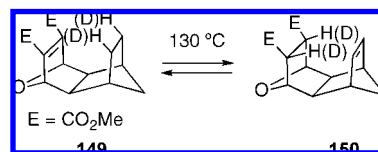


bond retards the 2H group-transfer, which indicates a truly pericyclic behavior for this transformation. Moreover, the activation parameters of the process are in the ranges of  $\Delta H^\ddagger = 25$  to  $33$  kcal/mol and  $\Delta S^\ddagger = \text{ca. } -8$  to  $-14$  cal/(K mol), indicating that type II dyotropic rearrangements exhibit activation values similar to those for type I dyotropic reactions.

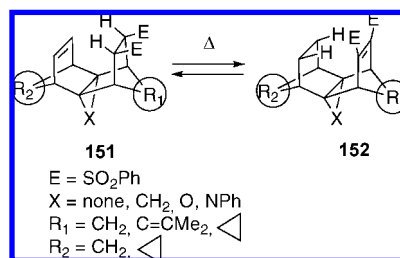
Kinetic and structural studies clearly show that the internuclear proximity  $d_{\text{CH}}$  as defined in Scheme 58 (also called *precompression*) is decisive for the process. Thus, changes in  $d_{\text{CH}}$  of only  $0.1$ – $0.17$  Å translate into a rate spread of  $10^4$  s $^{-1}$ . However, not only this structural parameter controls the transformation. Other factors, such as the reactant strain energy, also influence the reaction rate of the process. Moreover, the corresponding transition state of the process is particularly sensitive to incipient changes in the overall  $\pi$ -energies ( $\Delta E_\pi$ ) of the rearrangement. Small changes in  $\pi$ -energy at the receptor  $\pi$ -bond, occasioned by the proximity of polarizing substituents on the adjacent methylene bridge, contribute to the modest rate-spread observed for the series of trienes **145** (about an order of magnitude).<sup>105,106</sup> It is also worthy of note that while primary deuterium kinetic isotope effects in the rearrangements of compounds **147** reveal unambiguous evidence for a tunneling contribution to the kinetics, the analogous dyotropy of compounds **145** shows comparatively smaller tunneling components.<sup>105,107,108</sup>

Vogel and co-workers reported the thermally induced [ $\sigma 2_s + \sigma 2_s + \pi 2_s$ ] process in the *endo,endo*-11-oxatetracyclododecene derivative **149** (Scheme 60), a process similar to the rearrangement observed in isodrins **145**.<sup>109</sup> The thermochemical data [ $\Delta H^\ddagger = 35$ – $39$  kcal/mol and  $\Delta S^\ddagger = 2$ – $11$  cal/(K mol)] and the deuterium labeling experiments

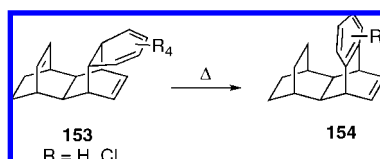
Scheme 60



Scheme 61



Scheme 62

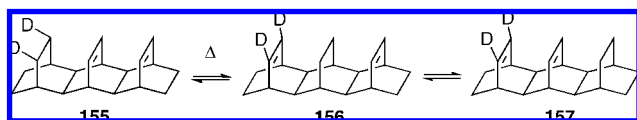


are consistent with a concerted intramolecular mechanism involving the stereospecific  $4,5\text{-endo} \rightleftharpoons 9,10\text{-endo}$  double hydrogen atom migration. Moreover, the rate constant of the rearrangement is not affected by the concentration, in agreement with the intramolecular nature of the process.

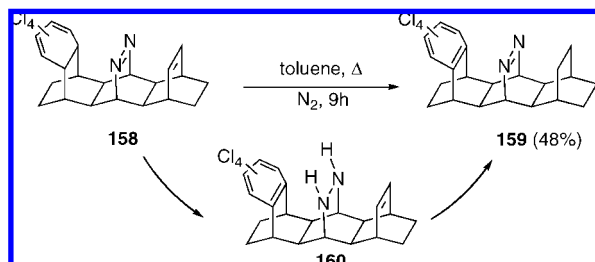
Paquette and co-workers reported the closely related type II dyotropic hydrogen transfer in *syn*-sesquinorbornene disulfones **151** (Scheme 61).<sup>110,111</sup> On the basis of extensive kinetic and structural studies, it was found that the considered intramolecular dyotropic reactions are not exclusively controlled by the distance between the migrating hydrogen atoms and the  $\pi$ -acceptor bond ( $d_{\text{CH}}$  in Scheme 58). In agreement with the findings by MacKenzie,<sup>105–108</sup> although the proximity of the reaction centers is clearly a prerequisite for smooth operation of the dyotropic shifts, the modulation of this distance is not the sole contributor to the reaction rate. Other key changes, which include but are not necessarily limited to, the differences in the energy required to stretch bonds, variations in the extent of strain release, changes in the freedom of motion, and dissimilarities in developing  $\pi$ -electronic effects, may determine the magnitude of the energy barrier and possible changes in the reaction thermodynamics.<sup>112</sup> Quantum chemical calculations on model compounds leave room for uncertainty about the reaction mechanism, namely whether the *endo*- $\alpha$ -sulfonyl hydrogen atoms migrate concertedly to the proximal double bond in a [ $\sigma 2_s + \sigma 2_s + \pi 2_s$ ] fashion or do so nonclassically through a stepwise mechanism, via a tunneling that would skirt the full energetic costs associated with the formation of biradical intermediates.<sup>113</sup>

Grimme and co-workers reported similar 2H-dyotropic transfers in dihydrosesqui- and dihydro-*syn*-sesterbicyclo[2.2.2]octenes **153** and **155**–**157** (Schemes 62 and 63).<sup>114</sup> Again, the kinetic data indicate that the activation parameters of the process are in the ranges  $\Delta H^\ddagger = 20$  to  $36$  kcal/mol and  $\Delta S^\ddagger = \text{ca. } -10$  to  $-18$  cal/(K mol). Therefore, they are similar to those found for the analogous hydrogen dyotropic shifts in the isodrin or isodrin-like frameworks (see above). A closely related process involving a double

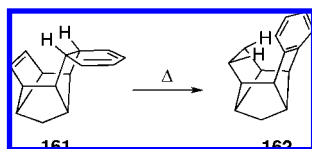
Scheme 63



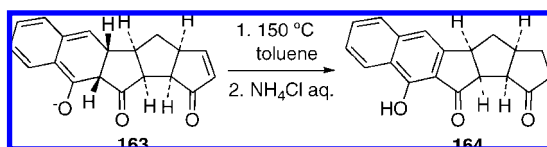
Scheme 64



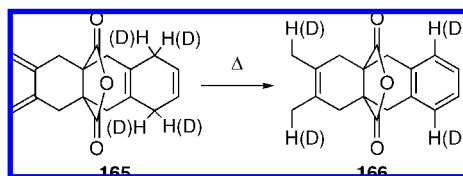
Scheme 65



Scheme 66



Scheme 67

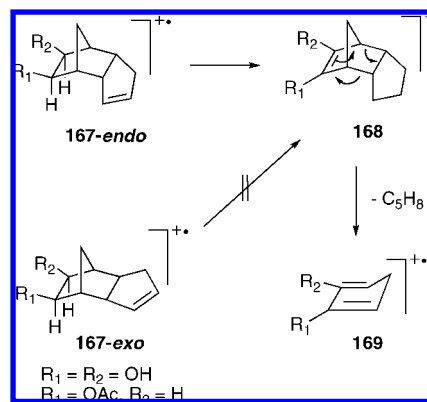


hydrogen migration with a N=N double bond as  $\pi$ -acceptor group has also been reported (Scheme 64).<sup>115</sup>

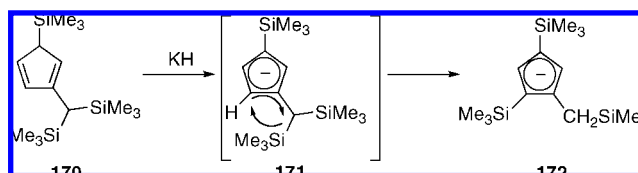
Other precompressed systems have been used as frameworks for the dyotropic transfer of hydrogen atoms. Chow and Ding reported the clean thermal conversion of pentacyclic diene **161** in its dyotropomer **162** (Scheme 65).<sup>116</sup> Similarly, the aromatization process has been invoked as the driving force for the dyotropic double hydrogen transfer from dione **163** to **164** (Scheme 66).<sup>117</sup> Finally, a first-order dyotropic transformation has been observed in the 2,3-bis(methylene)decahydroanthracene derivative **165** (Scheme 67).<sup>118</sup> Deuteration experiments as well as molecular mechanics calculations point to a concerted reaction mechanism for the latter process.

Double hydrogen dyotropic transfer also occurs in the gas-phase. Thus, the *endo* radical-cations **167** eliminate  $C_5H_8$  via a retro-Diels–Alder reaction (Scheme 68).<sup>119</sup> The process is hampered in the *exo* isomers. This highly stereospecific fragmentation requires a double hydrogen transfer in the molecular ions, which could take place in either a concerted or stepwise fashion. Field ionization kinetic experiments point to the concerted character of this double hydrogen dyotropic migration. This suggestion has been recently confirmed by means of density functional theory (DFT) calculations.<sup>120</sup>

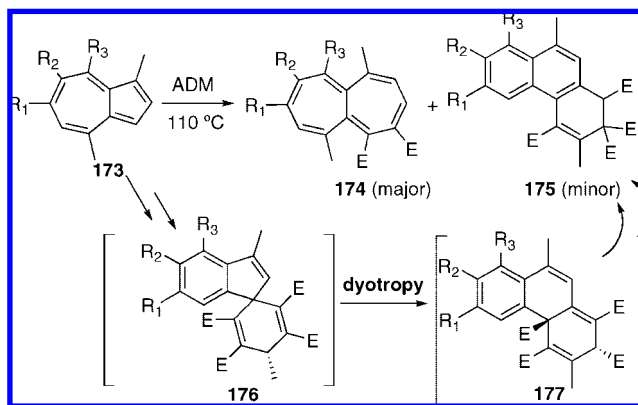
Scheme 68



Scheme 69



Scheme 70



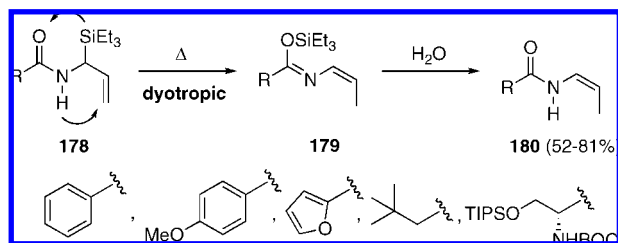
The presence of a rigid, precompressed skeleton is not necessarily a requisite for a type II dyotropic double group migration. Reaction on anion **171**, formed by desprotonation of **170** with KH, produces **172** via a type II dyotropic rearrangement. The process involves the 1,3-migration of the SiMe<sub>3</sub> group from the methyne carbon of the CH(SiMe<sub>3</sub>)<sub>2</sub> substituent with the concomitant reverse migration of a hydrogen atom (Scheme 69).<sup>121</sup> A concerted type II 8-dyotropic process has been proposed to explain the formation of the side-compounds **175** in the thermal reaction of azulenes **173** with dimethyl-acetylcendicarboxylate, ADM (Scheme 70).<sup>122</sup>

Danishefsky and Lin reported the transformation of *N*-( $\alpha$ -silyl)allyl amides **178** to *cis*-propenyl amides **180** upon heating and subsequent hydrolysis (Scheme 71) during the synthesis of proteasome inhibitor candidates TMC-95A and TMC-95B (see section 5.2).<sup>123</sup>

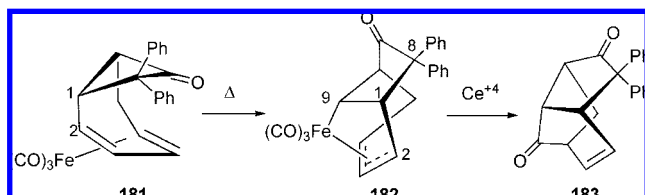
In contrast to the numerous reported type I dyotropic rearrangements involving transition metals (see section 2.2), reactions of type II involving metallic frameworks have been barely explored. Goldschmidt and Antebi reported a formal 1,3-diene to  $\sigma,\pi$ -allyliron–tricarbonyl dyotropic rearrangement (Scheme 72).<sup>124</sup> In this [2,2]-shift, the iron fragment, which is originally attached to the carbon atom in **181**, migrates to the neighboring carbon, forming the Fe–C<sub>9</sub>



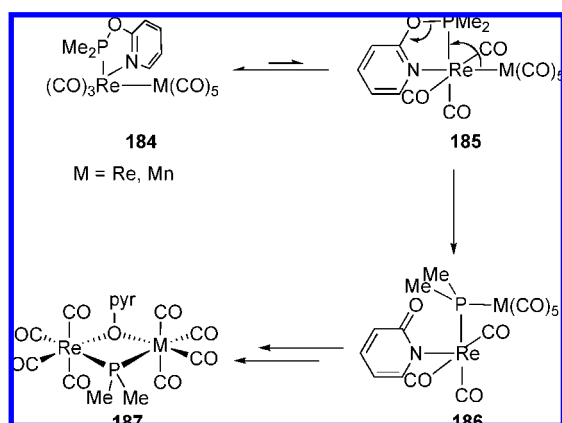
Scheme 71



Scheme 72



Scheme 73



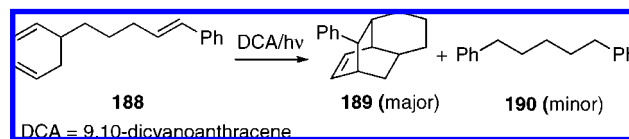
$\sigma$ -bond, while the diphenylcarbonyl carbon migrates from C<sub>1</sub> to C<sub>2</sub> to form the C<sub>1</sub>–C<sub>9</sub>  $\sigma$ -bond in **182**. Unless the inversion on iron occurs, the rearrangement has to involve a symmetry forbidden thermal reaction and, therefore, it may alternatively occur through the intermediacy of a polar zwitterion. Dyotropomer **182** can be further oxidized by treatment with cerium salts to produce highly condensed tricyclic ketones **183**.

Collum and co-workers reported the rearrangement of dinuclear complexes **184**, which upon heating at 80 °C in benzene rearrange to complexes **187** (Scheme 73).<sup>125</sup> It is proposed that dinuclear complexes **184** are in rapid equilibrium with complexes **185**, which are able to undergo the type II dyotropic reaction, forming complexes **186**. Complexes **186** finally afford the observed species **187**. The proposed type II dyotropic reaction mechanism is in agreement with the kinetic observations: first order kinetics with activation parameters of  $\Delta H^\ddagger = \text{ca. } 23 \text{ kcal/mol}$  and  $\Delta S^\ddagger = \text{ca. } -10 \text{ cal/(K mol)}$ .

### 3.2. Photochemical Reactions

Type II dyotropic rearrangements can also be induced by irradiation.<sup>126</sup> Thus, the 9,10-dicyanoanthracene (DCA) sensitized photolysis of a benzene solution of compound **188** gives two products in a ratio of 3:1 that are isomeric with the starting material (Scheme 74). The major product was identified as the *endo,trans*-tricyclic hydrocarbon **189** formed by an intramolecular Diels–Alder reaction. The dyotropic

Scheme 74



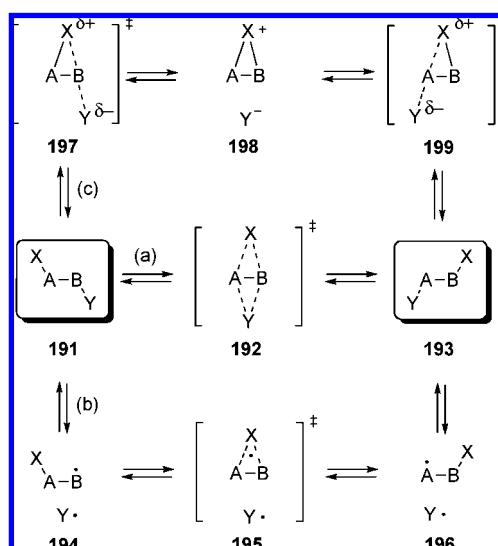
hydrogen transfer from the cyclohexene moiety to the acceptor styrene group forms the minor product **190**. This photochemically induced type II transformation may also occur stepwise by sequential transfer of the hydrogen atoms and formation of the corresponding radical intermediates. However, no experiments have been carried out to determine the concerted or stepwise nature of this process.

## 4. Theoretical and Computational Studies on Reaction Mechanisms

### 4.1. Type I Dyotropic Processes

Strictly speaking, dyotropic reactions are concerted and take place via cyclic transition structures. This situation corresponds to pathway (a) shown in Scheme 75, in which transition structure **192** is under orbital symmetry control. However, as it happens in pericyclic reactions such as cycloadditions and sigmatropic rearrangements, the dyotropic transformation from X–A–B–Y species **191** to the rearranged product Y–A–B–X **193** can alternatively take place via stepwise mechanisms involving ionic or radical species. Thus, homolytic cleavage of the B–Y bond can yield the radical pair **194** that rearranges to **196** via transition structure **195**, as is shown in pathway (b) of Scheme 75. Alternatively, if X has lone pairs available for intramolecular nucleophilic attack and Y is a good leaving group, formation of ionic pairs of type **198** could occur, whose ring aperture would yield the rearranged product **193** via pathway (c). In the subsequent subsections, examples of the mechanistic alternatives postulated in Scheme 75 will be discussed.

Scheme 75



#### 4.1.1. Concerted Pathways

If a type I dyotropic transformation involving a degenerate isomerization of a X–CH<sub>2</sub>–CH<sub>2</sub>–X molecule is considered, the corresponding D<sub>2h</sub>-symmetric transition structure (TS) will be that depicted in Figure 1.<sup>9</sup> The diagram corresponding

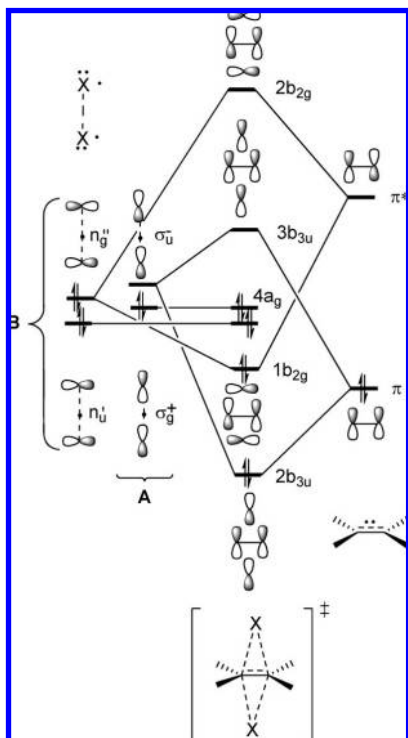
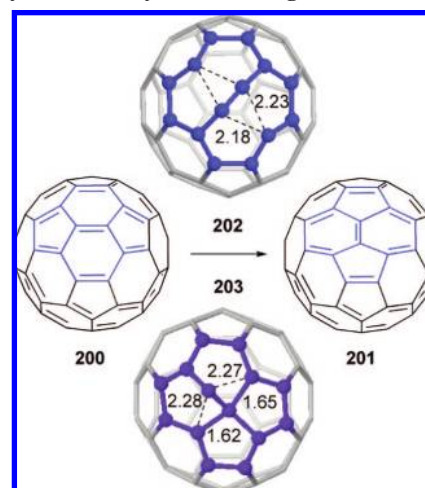


Figure 1.

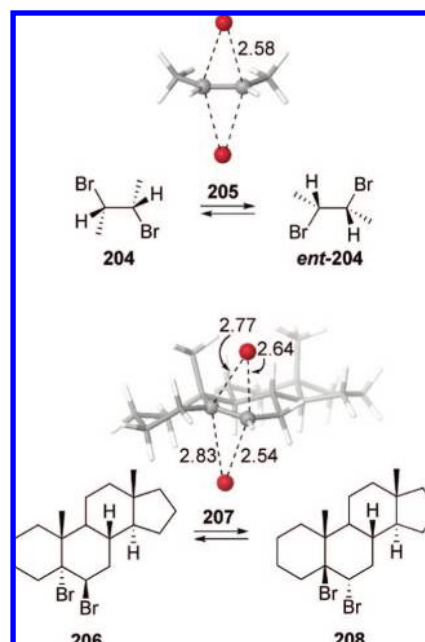
to the orbital interaction between the migrating X groups and the static ethylene subunit is also included in this figure. Examination of this diagram shows that if the migrating groups only interact with the static scaffold via the  $\sigma$ -set A, only the  $\sigma_u^-$  combination will interact with the  $\pi$  orbital, thus generating the occupied  $2b_{3u}$  MO, whereas the  $\sigma_g^+$  subunit remains unchanged. Therefore, if only the set A participates in the type I dyotropic rearrangement, a pericyclic TS is not possible and the reaction is symmetry forbidden. However, if X has an additional set of nonbonding electron pairs or  $\pi$ -symmetric subunits, the  $n_g''$  combination of the B-set shown in Figure 1 can interact with  $\pi^*$ , thus completing the cyclic electronic circulation required for a pericyclic mechanism (Figure 1).

The Stone–Wales rearrangement in fullerenes<sup>127</sup> belongs to this kind of transformations. This reaction consists of the rearrangement of  $I_h$ -symmetric buckminsterfullerene **200** to the  $C_{2v}$ -symmetric  $C_{60}$  isomer **201** (Scheme 76). A similar process has been investigated for  $C_{36}$ .<sup>128</sup> Two general mechanisms have been proposed: a concerted process according to mechanism (a) of Scheme 75 that involves a  $C_2$ -symmetric transition structure **202** (Scheme 76),<sup>129</sup> and a stepwise mechanism involving a nonplanar carbene intermediate.<sup>128,130</sup> High level calculations by Bettinger et al.<sup>131</sup> have shown that the first mechanism exhibits only the two-electron interaction involving the  $\pi$  and  $\sigma_u^+$  orbitals shown in Figure 1. As a consequence, transition structure **202** corresponds to a forbidden process. In addition, the same authors did not find a stepwise reaction path but a transition structure **203** that exhibits the carbene-like character. Both processes have very high activation energies (ca. 167 kcal/mol). It has been suggested that this high barrier can be lower in endohedral metallofullerenes.<sup>132</sup>

Using the A and B sets in the interaction scheme shown in Figure 1 should result in much lower activation energies. Under this framework, the dyotropic rearrangement of different vicinal dibromoalkanes has been studied.<sup>9</sup> Two

Scheme 76. Coordinates of Transition Structures **202** and **203** Kindly Provided by Prof. Bettinger (Ref 131)<sup>a</sup>

<sup>a</sup> Bond distances are given in angstroms (see the corresponding reference for computational details).

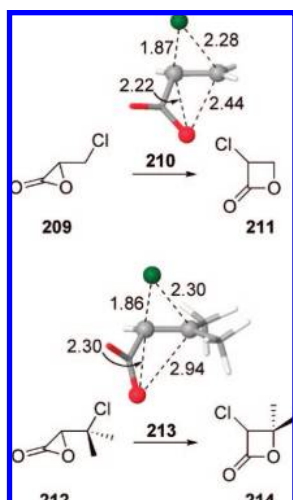
Scheme 77. Coordinates of Transition Structures **205** and **207** Taken from Ref 9<sup>a</sup>

<sup>a</sup> Bond distances are given in angstroms (see the corresponding reference for computational details).

representative examples are given in Scheme 77. In all cases, the geometric and energetic features of the concerted transition structures are in good agreement with this qualitative model. It is noteworthy that more asynchronous transition structures such as **207** possess an asymmetric charge distribution similar to that expected for intermediates such as **198** (Scheme 75, mechanism (c)).

Williams and co-workers<sup>133</sup> have described the transition structures associated with the dyotropic rearrangements of  $\beta$ -chloro- $\alpha$ -lactones **209** and **212** to  $\alpha$ -chloro- $\beta$ -lactones **211** and **214** (Scheme 78). The geometries of transition structures **210** and **213** in water are also depicted in this scheme. The authors found that these saddle points are quite polar, with considerable chloronium carboxylate character, which is related with intermediates **198** (Scheme 75, mechanism (c)). They also rationalize their results in terms of a double  $S_N2$ -

**Scheme 78.** Coordinates of Transition Structures **210** and **213** Have Been Taken from Ref 133<sup>a</sup>



<sup>a</sup> Bond distances are given in angstroms (see the corresponding reference for computational details).

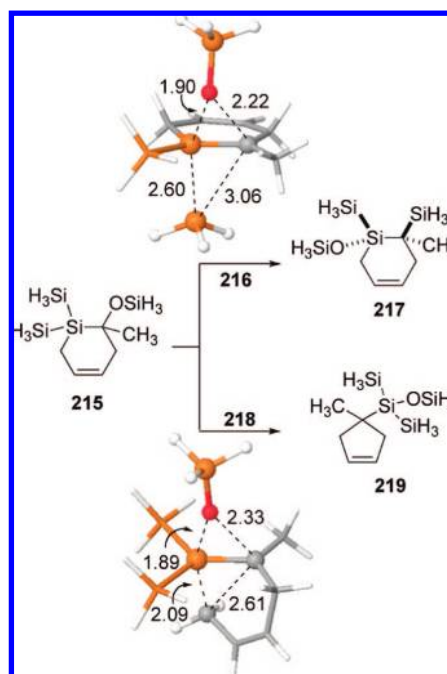
like reaction where the leaving group of one attack is the nucleophile for the other and *vice versa*, thus resulting in a concerted but highly asynchronous process, with the release of ring strain acting also as a driving force. Since the C<sub>β</sub> atom of both **210** and **213** has a significant carbocation character, the activation barrier for the **212** → **214** dyotropic reaction is lower than that computed for the reaction involving transition structure **210**.

This kind of geometries is also found when a C–Si moiety is the static scaffold. Thus, computations on model structures related to the arrangements gathered in Scheme 26 revealed that both the Si–O and Si–C rearrangements occur concertedly (but via asynchronous transition structures; see Scheme 79) with an activation barrier of ca. 43 kcal/mol for the **215** → **217** rearrangement (which is in the line of similar type I dyotropic processes).<sup>4</sup> The alternative **215** → **219** transformation involves the migration of one methylene and one silyloxy group via transition structure **218**. The computed activation barrier for this process was ca. 5 kcal/mol higher than that associated with transition structure **216**.<sup>50</sup>

Klingebl et al.<sup>71b</sup> have found similar geometries for transition structures associated with dyotropic rearrangements having a static N–O scaffold and two migrating silyl groups (Scheme 80). Thus, *O*-trifluoromethyl-*N,N*-bis(trimethylsilyl)hydroxylamine **220** irreversibly isomerizes to the *N*-trifluorosilyl derivative **222** via concerted transition structure **221** with a computed barrier of ca. 30 kcal/mol. The calculations indicate that the anomeric stabilization of **222** by more favorable negative F–Si–N and O–Si–C hyperconjugation is important for the course of the reaction.

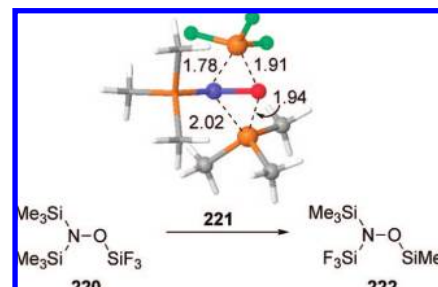
An interesting example of a type I dyotropic rearrangement involving a concerted (albeit highly asynchronous) hydrogen and carbon migration on a static C–C scaffold has been proposed for the biosynthesis of pentalene **227** from farnesyl diphosphate **223** (Scheme 81).<sup>134</sup> Carbocation **224** transforms stereospecifically into the more stable intermediate **226** via transition structure **225** with an activation barrier of ca. 30 kcal/mol (**225** is proposed to be stabilized by an intramolecular cation– $\pi$  interaction). Intermediate **226** is thence transformed into pentalene via a simple E1 pathway (Scheme 81).

**Scheme 79.** Coordinates of Transition Structures **216** and **218** Taken from Ref 50<sup>a</sup>



<sup>a</sup> Bond distances are given in angstroms (see the corresponding reference for computational details).

**Scheme 80.** Coordinates of Transition Structure **221** Taken from Ref 71b<sup>a</sup>



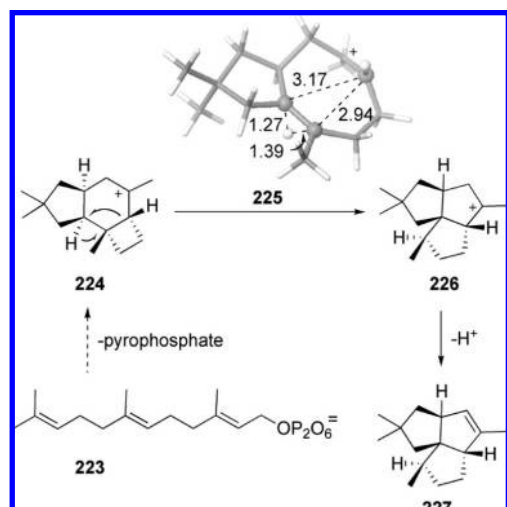
<sup>a</sup> Bond distances are given in angstroms (see the corresponding reference for computational details).

#### 4.1.2. Stepwise Mechanisms

Yu and Feng have reported theoretical studies on the thermal rearrangements of silylmethanamine **228** to form methylsilanamine **230** via a concerted transition state **229** or to form (methylamino)silane **234** through a stepwise mechanism. This stepwise mechanism involves transition structures **231** and **233** and the intermediate aminosilane–carbene complex **232** (Scheme 82).<sup>135–137</sup> These reactions are the model reactions for the dyotropic transformations shown in Scheme 27. The computed activation barrier for the concerted dyotropic rearrangement via transition structure **229** (corresponding to a mechanism of type (a), Scheme 75) has an activation barrier of 66.8 kcal/mol. In contrast, the **228** → **232** and **232** → **234** steps (corresponding to a mechanism of type (b), Scheme 75) have activation barriers of 59.2 and 12.4 kcal/mol, respectively. Interestingly, when the same reaction takes place with  $\alpha$ -silylalcohols, the mechanism of both dyotropic rearrangements is concerted.<sup>137</sup>

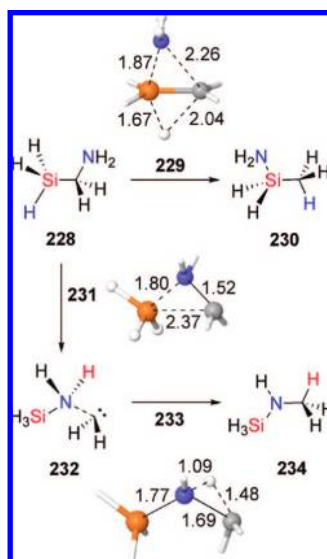
Similarly, the isomerization reactions indicated in Scheme 21 cannot proceed under physiologically available conditions and require catalysis by coenzyme B<sub>12</sub>-dependent enzymes.

**Scheme 81. Coordinates of Transition Structure 225 Taken from Ref 134<sup>a</sup>**



<sup>a</sup> Bond distances are given in angstroms (see the corresponding reference for computational details).

**Scheme 82. Coordinates of Transition Structures 229, 231, and 233 Taken from Ref 137<sup>a</sup>**

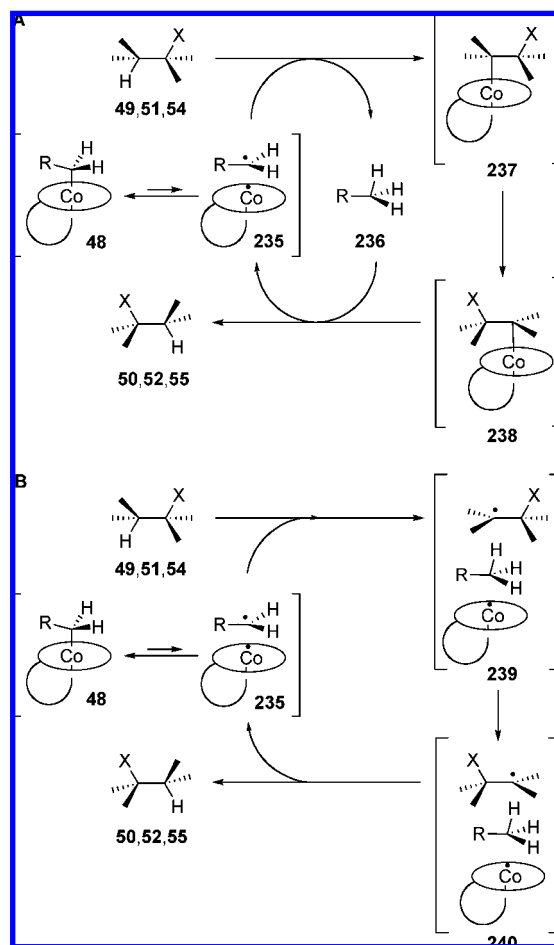


<sup>a</sup> Bond distances are given in angstroms (see the corresponding reference for computational details).

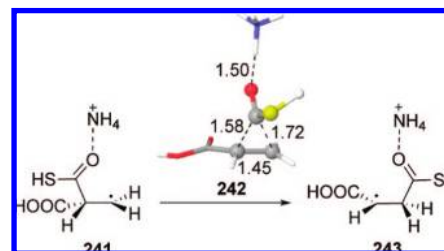
Two general stepwise pathways to isomerize reactants **49**, **51**, and **54** (Scheme 21) to products **50**, **52**, and **55** can be envisaged. Pathway A in Scheme 83 involves the initial homolytic dissociation of cofactor **48** to yield **235**. The reactions of substrates **49**, **51**, and **54** with **235** form the organometallic intermediate **237** and deoxyadenosine **236**. The 1,2-dyotropic rearrangement occurs in intermediate **237** and leads to cofactor bounded products **238**. The reaction products **50**, **52**, and **55** are released by homolytic recombination of **236** with **238** to regenerate the cofactor **48**.<sup>138</sup>

Pathway B in Scheme 83 may be considered as an extension of the stepwise mechanism (b) shown in Scheme 75. Now, the radical moiety of intermediate **239** isomerizes to **240** with no covalent interaction with the deoxyadenosine–cobalamin complex. Hydride radical recombination within **240** complex yields the reaction products, in a process which occurs with double inversion of configuration and concomitant recovery of cofactor **48**.

**Scheme 83**



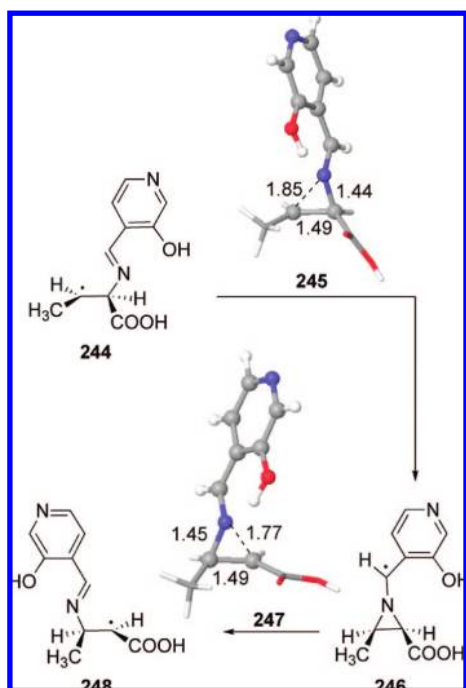
**Scheme 84. Coordinates of Transition Structure 242 Taken from Ref 141<sup>a</sup>**



<sup>a</sup> Bond distances are given in angstroms (see the corresponding reference for computational details).

The model depicted as pathway B in Scheme 83 has proven to be compatible with experimental results,<sup>139</sup> and it has been used in many computational studies.<sup>140</sup> Thus, Radom and co-workers<sup>141</sup> have found that the key step in the isomerization of (*R*)-methylmalonyl-CoA is a radical isomerization facilitated by a basic residue of methylmalonyl-CoA mutase (presumably His244), as is shown in the model transformation gathered in Scheme 84. Transition structure **242** is referable to the transition structure of type **195** (Scheme 75) but not to a concerted dyotropic rearrangement of a Co-bound intermediate such as **237** (Scheme 83). This assistance by positively charged residues has also been observed in diol dehydratase, in which a synergistic retro-push–pull effect induced by acidic, basic, and metallic residues promotes a significant lowering of the activation barrier.<sup>142</sup>



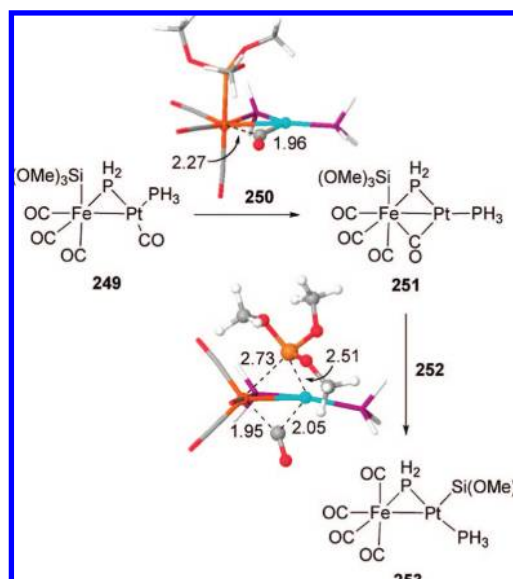
**Scheme 85. Coordinates of Transition Structures 245 and 247 Taken from Ref 143<sup>a</sup>**

<sup>a</sup> Bond distances are given in angstroms (see the corresponding reference for computational details).

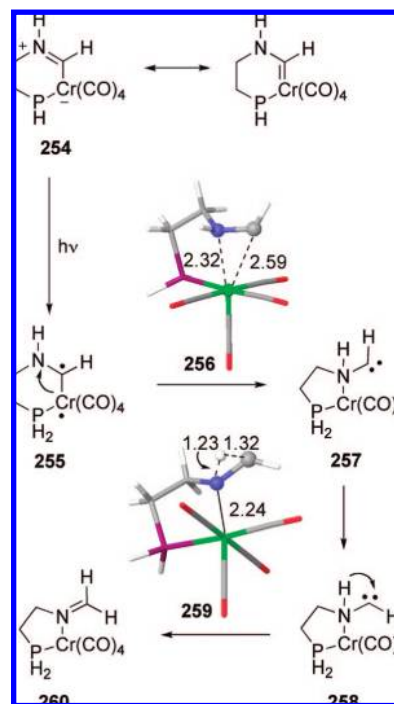
A slightly different mechanism has been proposed on the basis of computational results for the reactions catalyzed by the B<sub>12</sub>-dependent enzymes lysine 2,3-aminomutase and lysine 5,6-aminomutase. These enzymes also use pyridoxal 5'-phosphate as cofactor, and the resulting intermediate Schiff bases **244** isomerize to product-like radicals **248** via formation of intermediate *N*-benzylaziridine radicals of type **246**.<sup>143</sup> Therefore, in this case mechanism (b) depicted in Scheme 75 is modified by the presence of ring-opening/-closing transition structures **245** and **247** (Scheme 85).

Stepwise mechanisms have also been proposed for structures involving bimetallic static moieties. Thus, computational studies on model Fe–Pt heterodimetallic compounds **249** have shown that, in the double migration of CO and silyl groups, there is a previous migration of one CO from Pt toward Fe to form a  $\mu^2$ -CO intermediate **251** (Scheme 86).<sup>92</sup> This local minimum **251** proceeds to the rearranged compound **253** via transition structure **252**, which apparently corresponds to a concerted mechanism of type (a) (Scheme 75).

The photochemically induced stepwise dyotropic reaction of certain cyclic Fischer carbenes has been also reported (Scheme 56).<sup>95–97</sup> A computationally tractable model is reported in Scheme 87. Carbene **254** yields *N*-coordinated imine **260** upon irradiation. The rearrangement occurs on the triplet potential energy surface by migration of the chromium atom from the carbon to the nitrogen atom, yielding an intermediate carbene species **257** via transition structure **256**. Rotation about the N–C bond and subsequent 1,2-prototropy yields the rearranged product via transition structure **259**. This mechanism was found to be in agreement with the experimental findings.<sup>95–97</sup>

**Scheme 86. Coordinates of Transition Structures 250 and 252 Taken from Ref 92<sup>a</sup>**

<sup>a</sup> Bond distances are given in angstroms (see the corresponding reference for computational details).

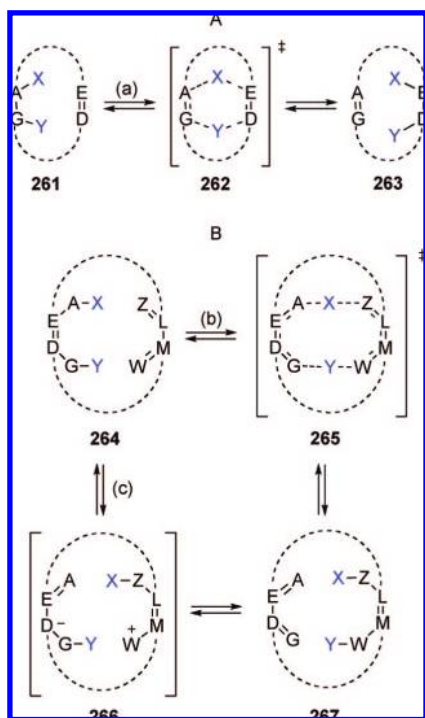
**Scheme 87. Coordinates of Transition Structures 256 and 259 Taken from Ref 95<sup>a</sup>**

<sup>a</sup> Bond distances are given in angstroms (see the corresponding reference for computational details).

## 4.2. Type II Dyotropic Reactions

These reactions can take place on different scaffolds, depending on the nature of the  $\pi$ -system and the number of atoms involved (Scheme 88). Thus, molecules having arrangements such as **261** can rearrange to compounds **263** via a six-membered transition structure **262** (Scheme 88, pathway (a)). Alternatively, more extended  $\pi$ -systems **264** can rearrange to unsaturated compounds **267**, either through concerted mechanisms involving transition structures such as **265** or through stepwise mechanisms involving zwitteri-

Scheme 88



onic species of type **266** (Scheme 88, paths (b) and (c), respectively). Dyotropic reactions involving (trialkylsiloxy)-enones<sup>144</sup> belong formally to the transformation reported in Scheme 88B, although no computational studies on the reaction mechanisms of these rearrangements have been reported to date.

#### 4.2.1. Concerted Pathways: Synchronicity and Aromaticity

A MO-based analysis has been reported for systems such as **261** in which  $X = Y = H$  (Figure 2).<sup>145</sup> When the model structure corresponds to two ethylene units and two hydrogen atoms arranged in a  $D_{2h}$ -symmetric system, the perturbed MOs associated with a double hydrogen transfer are those depicted schematically in Figure 2. The  $\pi_+$  combination of bonding MOs of ethylene interacts with the  $\sigma_g^+$  component to yield two  $a_{1g}^+$  MOs. Similarly, the  $\pi^* - \sigma_u^-$  combination yields two  $a_{2u}^+$  symmetric MOs, with the  $\pi_-$  combination

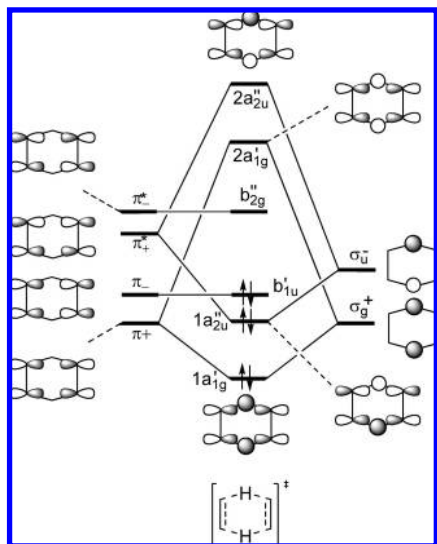
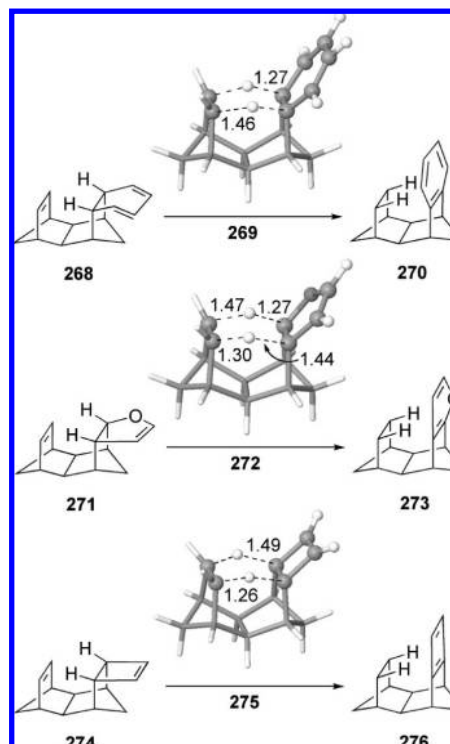


Figure 2.

Scheme 89. Coordinates of Transition Structures **269**, **272**, and **275** Taken from Ref 146<sup>a</sup>

<sup>a</sup> Bond distances are given in angstroms (see the corresponding reference for computational details).

remaining essentially unchanged and becoming the  $b_{1u}^-$ -symmetric LUMO of this model transition state. Therefore, this model double-hydrogen transfer involves six electrons in a cyclic arrangement and is symmetry allowed. Indeed, it has been reported<sup>145</sup> that the MOs shown in Figure 2 are the in-plane equivalent of the MOs of stable aromatic molecules.

The structures of the concerted transition structures associated with different dyotropic reactions have been reported (Scheme 89).<sup>113,146</sup> These rearrangements have been described as highly synchronous transformations that take place via in-plane aromatic transition structures similar to **262** (Scheme 88A). Some examples are given in Scheme 89.

The driving force for these processes is the aromaticity of the final products. Thus, reaction **268**  $\rightarrow$  **270** has a calculated activation barrier of only 19.9 kcal/mol, with the corresponding reaction energy being  $-41.1$  kcal/mol. Similarly, reaction **271**  $\rightarrow$  **273** has calculated barrier and reaction energies of 36.6 and  $-6.8$  kcal/mol, respectively. In contrast, the **274**  $\rightarrow$  **276** transformation exhibits a late transition state **275**, with the calculated barrier and reaction energies being 63.3 and 46.6 kcal/mol, respectively (Scheme 89). Since the reactions gathered in Scheme 89 involve formation of substituted benzene, furan, and cyclobutadiene (archetypal examples of aromatic and antiaromatic compounds), it has been suggested that the activation and reaction energies of concerted type II dyotropic reactions similar to those depicted in Scheme 89 may be used to quantify the aromatic stabilization of cyclic molecules. Thus, excellent linear correlations between activation and reaction energies and aromatic stabilization energies (ASE)<sup>147</sup> were found (Figure 3).<sup>146</sup>

A double hydrogen transfer has been located computationally in the thermal dimerization of cyclopropenes (Scheme 90).<sup>148</sup> The features of transition structure **278**, resulting from

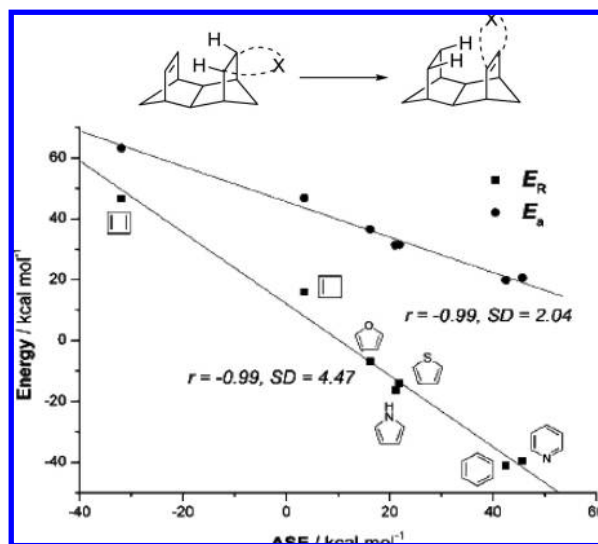
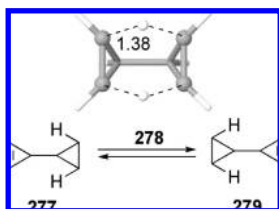


**Figure 3.** Plot of the ASE values vs the activation ( $E_a$ , circles) and reaction ( $E_R$ , squares) energies for different dyotropic reactions involving aromatic, nonaromatic, and antiaromatic molecules.<sup>146</sup>

the degenerate dyotropic rearrangement of **277**, are similar to those found for saddle points **269**, **272**, and **275**. However, the computed activation energy (52.1 kcal/mol) for the rearrangement of **277** is higher than in the cases where the formation of aromatic species in the final products is involved in one cyclic moiety.

**Scheme 90.** Coordinates of Transition Structure **278** Taken from Ref 148<sup>a</sup>

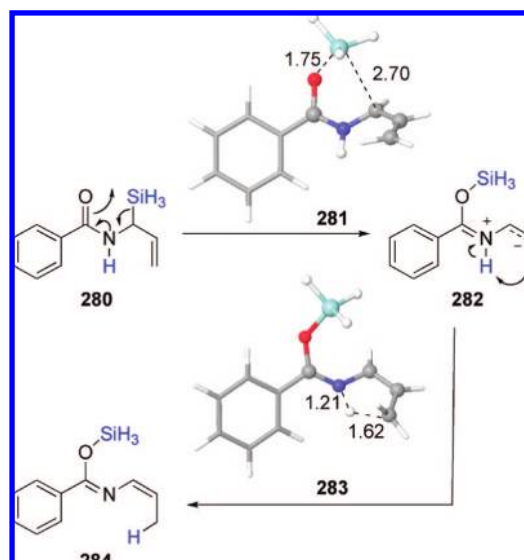


<sup>a</sup> Bond distances are given in angstroms (see the corresponding reference for computational details).

#### 4.2.2. Stepwise Pathways

To date, the single paper reporting a computational study on stepwise type II dyotropic reactions was reported by Houk, Danishefsky, and co-workers<sup>149</sup> on model system **280** for the transformation depicted in Scheme 91. This process involves a 1,4-silyl migration coupled with a 1,4-hydrogen shift, and therefore, it can be considered as a formal 10-electron type II dyotropic rearrangement. DFT calculations reveal that the first step of the transformation of **280** to the product **284** (Scheme 91) involves the formation of intermediate **282** by the 1,4-migration of the silyl group to the oxygen atom via transition structures such as **281**. Intermediate **282** is then transformed to the final product by a 1,4-hydrogen shift through transition structure **283** (Scheme 91). The competitive concerted mechanism is hampered, since it is highly demanding in terms of geometric organization for the corresponding concerted transition state. Moreover, the stability of the 1,3-dipolar azomethine ylide intermediate **282** (formally equivalent to zwitterionic intermediate **266**, Scheme 88B, path (c)), which profits from charge stabilization by allylic resonance and phenyl conjugation, favors the stepwise pathway. In fact, the analogous intermediate formed after

**Scheme 91.** Coordinates of Transition Structures **281** and **283** Taken from Ref 149<sup>a</sup>



<sup>a</sup> Bond distances are given in angstroms (see the corresponding reference for computational details).

the 1,4-hydrogen migration as the first step of the transformation is computed to be highly unstable and would instantly convert into another product, which was not observed experimentally. The initial migration of the silyl moiety over the hydrogen group agrees with the well-documented higher migratory abilities of silyl groups compared to hydrogen atom.<sup>150</sup> An additional factor favoring the initial silyl group migration is the facile formation of azomethine ylides by 1,2-silyl shifts.<sup>151</sup>

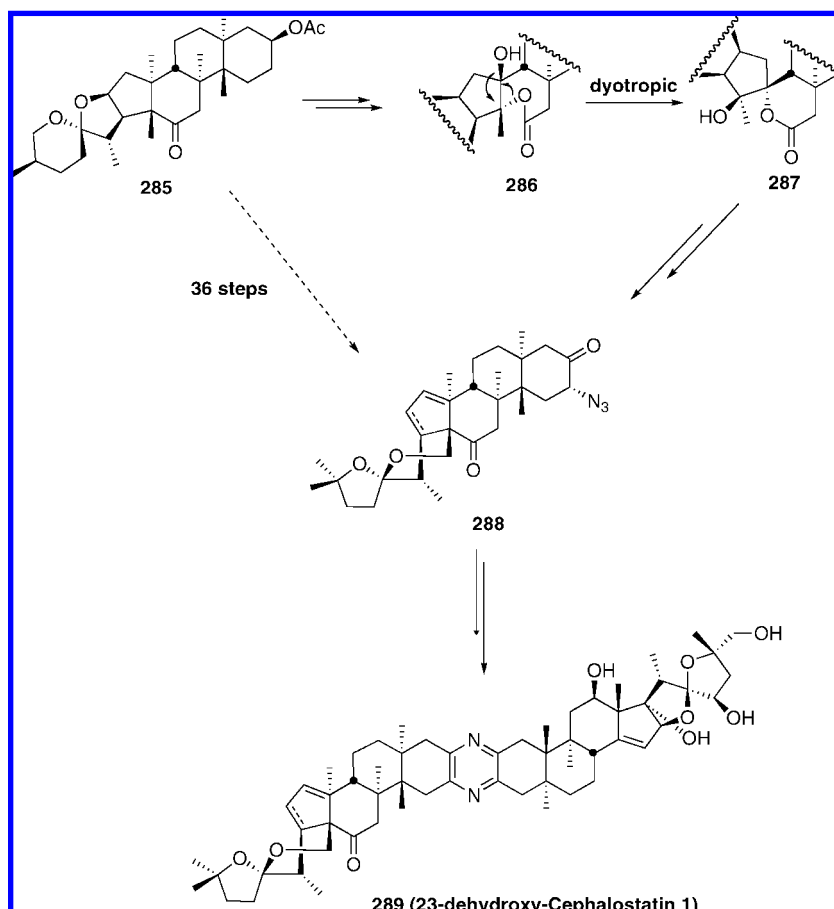
## 5. Applications of Dyotropic Rearrangements in Total Synthesis

The deep changes in the molecular skeleton derived from a dyotropic rearrangement resulted in powerful synthetic transformations. Hence, it is not surprising that dyotropic transformations have been used in the construction of complex molecules, since they allow introduction of structural features which are difficult, when not impossible, to obtain using other synthetic procedures. The following examples clearly illustrate the synthetic usefulness of these processes.

### 5.1. Synthesis of 23'-Deoxy Cephalostatin 1-Analogues

The first-generation synthesis of South 1 subunit **288** of cephalostatin analogues requires 36 operations from **285**, which makes this approach unattractive on the strategic level. However, Fuchs and co-workers have recently reported a remedy to this shortcoming.<sup>152</sup> Thus, one of the key steps of the new strategy involves the stereospecific 1,2-type I dyotropic rearrangement of **286** to spiro lactone **287** (Scheme 92). The transformation provokes the contraction of seven-membered fused lactones to their more stable spiro 6-ring counterparts.<sup>153</sup> Subsequently, the total synthesis of 23'-deoxycephalostatin was accomplished in only 16 operations with an overall yield of 9%. This clear reduction of the number of steps necessary to accomplish the synthesis of

## Scheme 92



the target molecule definitely shows the synthetic power of dyotropic reactions.

## 5.2. Synthesis of the Proteasome Inhibitors TCM-95A and TCM-95B

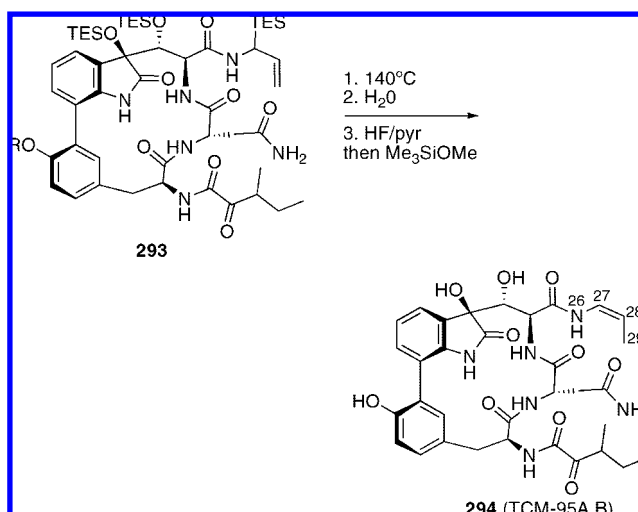
The type II dyotropic reaction of  $\alpha$ -silylallyl amides to produce *cis*-propenyl amides (Scheme 71) constitutes the key step during the synthesis of cyclic peptides TCM-95A and TCM-95B. This transformation was successfully applied in the final steps of the synthesis of the target molecules TCM-95A,B to accomplish the stereospecific *cis*-propenyl amide formation (Scheme 93).<sup>123</sup>

## 5.3. Applications of the Dyotropic Rearrangement of 5-Lithiodihydrofurans in Total Synthesis

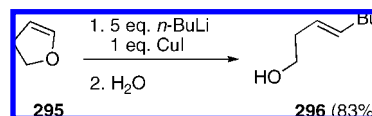
Sato and co-workers reported that the reaction of dihydrofuran **295** with *n*-BuLi (5 equiv) in the presence of CuI (1 equiv) gave the *trans*-homoallylic alcohol **296** in 83% yield with high stereoselectivity and therefore proceeded with inversion of configuration (Scheme 94).<sup>154</sup> A possible reaction mechanism, postulated by Kocienski and co-workers, involves a formal type I 1,2-dyotropic rearrangement of the high order cuprate **298** to cuprate **299**, which can further react with electrophiles to stereoselectively produce trisubstituted alkenes (Scheme 95).<sup>155,156</sup>

This transformation has been profusely used in the synthesis of natural products.<sup>156</sup> The synthesis of the anti-hypotensive agent Lacrimin A (Scheme 96) provided the first significant application of the Cu(I)-catalyzed dyotropic 1,2-migration to the construction of complex molecules.<sup>157</sup> The

## Scheme 93



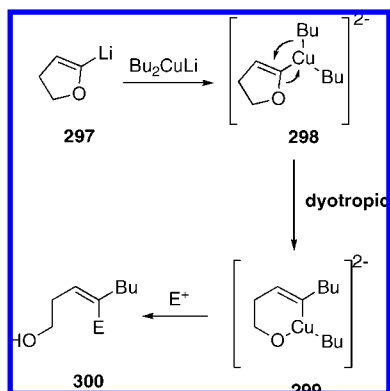
## Scheme 94



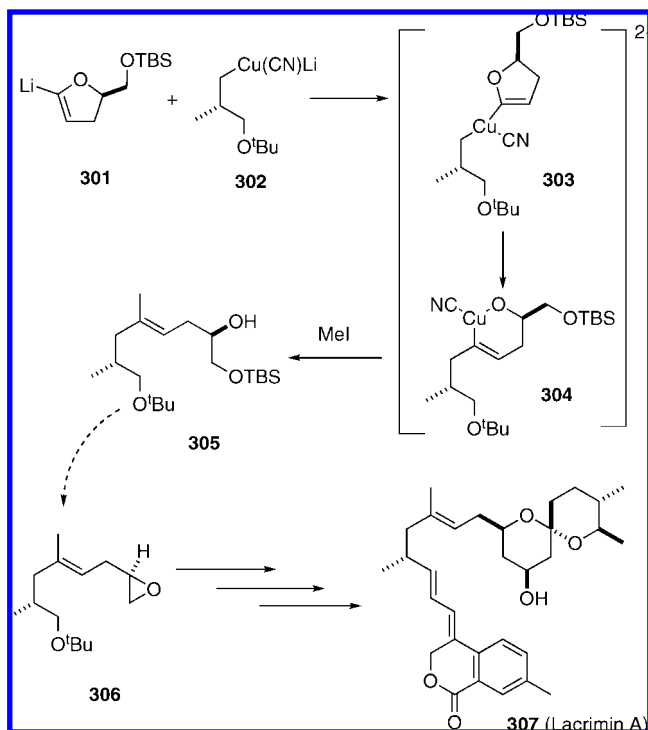
trisubstituted alkene intermediate **305** was generated by a sequence of reactions beginning with the formation and rearrangement of higher order cuprate **303**. The putative oxycuprate **304** was quenched with MeI to give the alkene **305** in 29% overall yield, which was further transformed to the precursor of Lacrimin A.



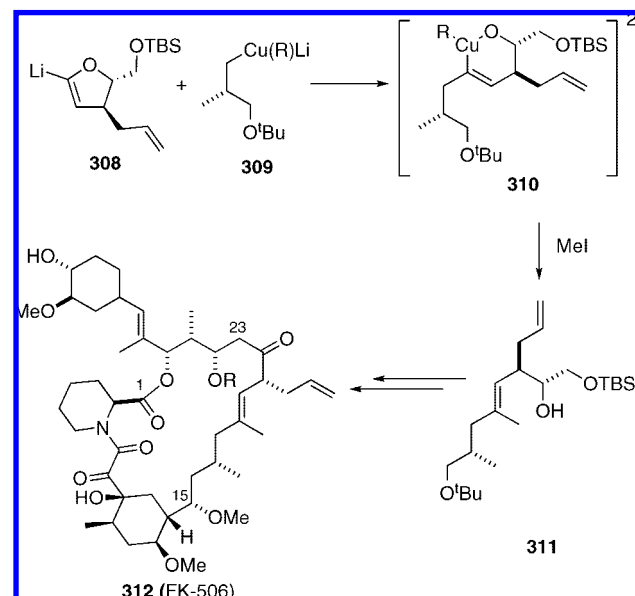
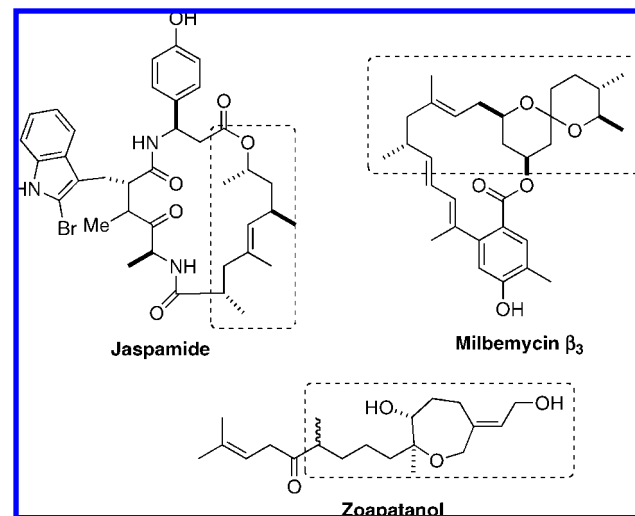
Scheme 95



Scheme 96



Scheme 97

Chart 1. Jaspamide,<sup>156</sup> Milbemycin  $\beta_3$ ,<sup>159</sup> and Zoapatanol<sup>a</sup>

<sup>a</sup> The dotted box indicates the fragment of the molecule which has been constructed by a 1,2-dyotropic rearrangement.

The synthesis of the C16–C23 fragment **311** of the potent immunosuppressive agent FK-506 was achieved (Scheme 97)<sup>158</sup> by reaction of the lithiated dihydrofuran **308** with the homocuprate **309**. This reaction forms the oxycuprate **310** via the expected 1,2-dyotropic rearrangement, which affords the desired trisubstituted alkene **311** in ca. 50% overall yield on quenching with MeI in the presence of HMPA. These transformations exemplify the value of the method for the construction of trisubstituted alkenes in sterically encumbered environments.

Different applications of the same Cu-promoted 1,2-dyotropic rearrangement based methodology by Kocienski's group also include the synthesis of the polyketide fragment 47 of the antifungal cyclodepsipeptide Jaspamide,<sup>156</sup> the precursor of Milbemycin  $\beta_3$ ,<sup>159</sup> and the total synthesis of the natural product Zoapatanol (Chart 1).<sup>160</sup>

Recently, Betzer, Ardisson, and co-workers applied a similar procedure toward the total synthesis of Discodermolide,<sup>161,162</sup> The C8–C14 subunit of Discodermolide possesses a trisubstituted *Z* double bond which is in principle readily accessible by a Cu-promoted 1,2-dyotropic rearrangement from the 5-lithiodihydrofuran **313**. Thus, the

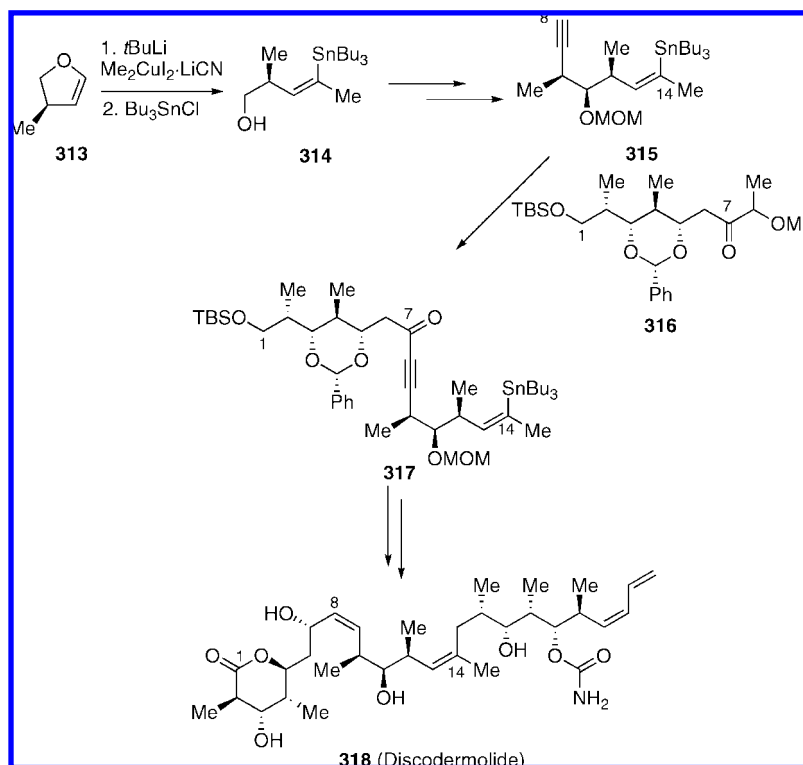
addition of  $\text{Me}_2\text{CuLi}\cdot\text{LiCN}$  and subsequent trapping with tri-*n*-butyltin chloride as electrophile result in the stereoselective formation of the unique *Z*-vinyltin derivative **314** in an optimized yield of 68%. Compound **314** is further transformed in **315**, which after reaction with **316** is converted in the Discodermolide precursor **317** (Scheme 98).

Interestingly, it has been proposed that the above dyotropic rearrangement is not restricted to Cu-compounds but also to boron,<sup>163</sup> zinc,<sup>164</sup> zirconium,<sup>165</sup> or aluminum.<sup>166</sup> However, there are few mechanistic details available and no firm evidence to suggest that all metallates abide by the same formal type I dyotropic mechanism.<sup>156</sup>

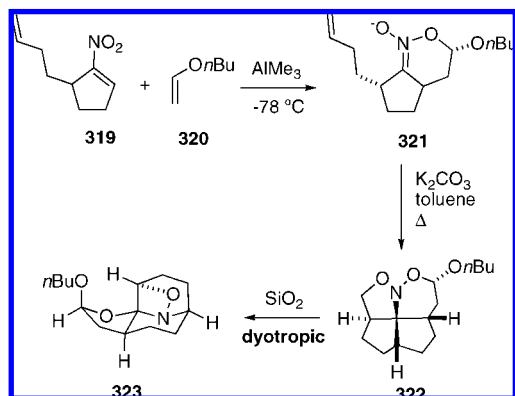
#### 5.4. Synthesis of Azafenestrane

During the synthesis of azafenestrans **326**, Denmark and co-workers<sup>167,168</sup> reported an unexpected dyotropic transformation which hampers the synthesis of the target molecule. The initial retrosynthetic plan involves the formation of nitrosoacetal **321** from the [4 + 3]/[3 + 2] tandem cycload-

Scheme 98



Scheme 99

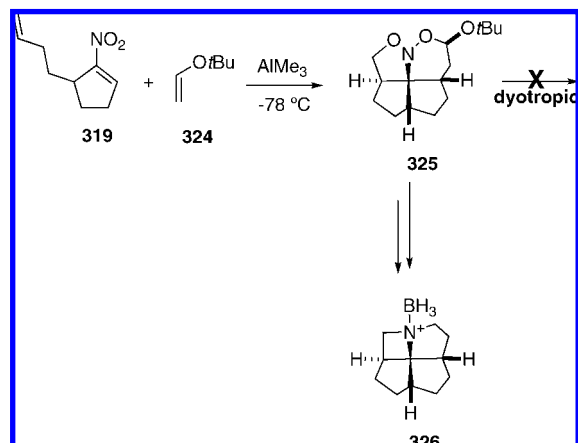


dition of nitroalkene **319** and vinyl ether **320**. Compound **321** is easily transformed in **322**, which in the presence of  $\text{SiO}_2$  unexpectedly rearranges to **323** at room temperature (Scheme 99). This process is a type I 1,2-dyotropic rearrangement, which obviously is favored due to the anticoplanar relationship between the migrating fragments. In order to overcome this problem and form azafenestrane, the authors used the bulkier vinyl ether **324**, which ensures the formation of nitrosoacetal **325**. The conformation of the latter compound avoids the possibility of the undesired dyotropic rearrangement and allows the synthesis of the target molecule (Scheme 100).

## 6. Conclusions and Outlook

Reetz in his review in 1977<sup>4</sup> stated “...The purpose of this chapter is not only to describe the present author’s own systematic studies involving organosilicon compounds, but also to motivate others in investigating dyotropic processes in general”. This review compiled the substantial advances made in the study of these processes, especially in their scope

Scheme 100



and mechanisms. In our opinion, Reetz’s purpose is three decades later fully accomplished. The herein discussed advances in these transformations have extended the initial view of dyotropic reactions as thermally induced and concerted processes to new photochemical reactions, involving transition metals and in many cases occurring by stepwise mechanisms. As one reviewer rightfully pointed out, “dyotropic reactions have been developed from exotic reactions into very useful tools for the construction of organic and organometallic molecules with interesting properties”. However, the search for new dyotropic transformations in general and particularly the study of the reaction mechanisms of these intramolecular reactions continue unabated. The synthetic potential of these processes is far from being mature, and in many cases this unique rearrangement may solve essential steps to prepare target molecules. We will use again the words by Reetz and conclude, hoping that this review motivates researchers in investigating new dyotropic processes in general and, in particular, in developing the full

potential of these rearrangements in organic and organometallic synthesis.

## 7. Acknowledgments

The authors thank the Spanish Ministerio de Educación y Ciencia (Grants CTQ2007-67730-C02-01/BQU, CTQ2007-67528/BQU and Consolider-Ingenio 2010, CSD2007-00006) for financial support. Financial support by the Gobierno Vasco-Eusko Jaurlaritza to F.P.C. (Grant IT-324-07) and the Comunidad Autónoma de Madrid to M.A.S. (Grant CAM CCG07-UCM/PPQ2595) is also gratefully acknowledged. I.F. is a Ramón y Cajal Fellow.

## 8. References

- Reetz, M. T. *Angew. Chem., Int. Ed. Engl.* **1972**, *11*, 129.
- Reetz, M. T. *Angew. Chem., Int. Ed. Engl.* **1972**, *11*, 131.
- Reetz, M. T. *Tetrahedron* **1972**, *29*, 2189.
- Reetz, M. T. *Adv. Organomet. Chem.* **1977**, *16*, 33.
- Grob, C. A.; Winstein, S. *Helv. Chim. Acta* **1952**, *35*, 782.
- Barton, D. H. R.; Head, A. J. *J. Chem. Soc.* **1956**, 932.
- Barili, P. L.; Bellucci, G.; Berti, G.; Marioni, F.; Marsili, A.; Morelli, I. *Chem. Comm.* **1970**, 1437.
- Grenier-Loustalot, M. F.; Lectard, A.; Metras, F. *Org. Magn. Reson.* **1975**, *7*, 376.
- Fernández, I.; Sierra, M. A.; Cossío, F. P. *Chem.—Eur. J.* **2006**, *12*, 6323.
- Frontera, A.; Suñer, G. A.; Deyá, P. M. *J. Org. Chem.* **1992**, *57*, 6731.
- Zou, J.-W.; Yu, C.-H. *J. Phys. Chem. A* **2004**, *108*, 5649.
- Mulzer, S.; Brüntrup, A. G. *Angew. Chem., Int. Ed. Engl.* **1979**, *18*, 793.
- Zenk, P. C.; Wiley, R. A. *Synthesis* **1984**, 695.
- Selected reviews on Wagner–Meerwein rearrangements: (a) Popp, F. D.; McEwen, W. E. *Chem. Rev.* **1958**, *58*, 375. (b) Cargill, R. L.; Jackson, T. E.; Peet, N. P.; Pond, D. M. *Acc. Chem. Res.* **1974**, *7*, 106. (c) Olah, G. A. *Acc. Chem. Res.* **1976**, *9*, 41. (d) Hogeveen, H.; Van Krutchten, E. M. G. A. *Top. Curr. Chem.* **1979**, *80*, 89. (e) Hanson, J. R. *Comp. Org. Synth.* **1991**, *3*, 705.
- Black, T. H.; Fields, J. D. *Synth. Commun.* **1988**, *29*, 1747.
- Miyashita, M.; Yamaguchi, R.; Yoshikoshi, A. *J. Org. Chem.* **1984**, *49*, 2857.
- Podraza, K. F.; Sneden, A. T. *J. Nat. Prod.* **1985**, *48*, 792.
- Black, T. H.; DuBay, W. J., III. *Tetrahedron Lett.* **1987**, *28*, 4787.
- Black, T. H.; Hall, J.; Sheu, R. G. *J. Org. Chem.* **1988**, *53*, 2371.
- Black, T. H.; DuBay, W. J., III. *Tetrahedron Lett.* **1988**, *29*, 1747.
- Mulzer, J.; Pomtner, A.; Strasser, R.; Hoyer, K.; Nagel, U. *Tetrahedron Lett.* **1995**, *36*, 3679.
- Black, T. H.; McDermott, T. S. *J. Chem. Soc., Chem. Commun.* **1991**, 184.
- Black, T. H.; Eisenbeis, S. H.; McDermott, T. S.; Maluleka, S. L. *Tetrahedron* **1990**, *46*, 2307.
- Black, T. H.; Hall, J. A.; Sheu, R. G. *J. Org. Chem.* **1988**, *53*, 5922.
- Arrastia, I.; Lecea, B.; Cossío, F. P. *Tetrahedron Lett.* **1996**, *37*, 245.
- Purohit, V. C.; Matla, A. S.; Romo, D. *J. Am. Chem. Soc.* **2008**, *130*, 10478.
- (a) Stöckner, F.; Käßlinger, C.; Beckert, R.; Görls, H. *Synlett* **2005**, *4*, 643. (b) Stöckner, F.; Beckert, R.; Gleich, D.; Birckner, E.; Günther, W.; Görls, H.; Vaughan, G. *Eur. J. Org. Chem.* **2007**, *8*, 1237.
- Wanzlick, H.-W.; Kleiner, H.-J.; Lasch, I.; Földner, H. U.; Steinmaus, H. *Liebigs Ann. Chem.* **1967**, *708*, 155.
- Hill, J. H. M. *J. Org. Chem.* **1963**, *28*, 1931.
- Sato, K.; Yamashita, Y.; Mukai, T. *Tetrahedron Lett.* **1981**, *22*, 5303.
- Hupe, E.; Denisenko, D.; Knochel, P. *Tetrahedron* **2003**, *59*, 9187, and references therein.
- Köster, R.; Seidel, G.; Boese, R.; Wrackmeyer, B. *Chem. Ber.* **1990**, *123*, 1013.
- (a) Banerjee, R.; Ragsalade, S. W. *Annu. Rev. Biochem.* **2003**, *72*, 209. (b) Toraya, T. *Cell. Mol. Life Sci.* **2000**, *57*, 106. (c) Banerjee, R. *Chem. Rev.* **2003**, *103*, 2083. (d) Toraya, T. *Chem. Rev.* **2003**, *103*, 2095.
- Buckel, W.; Golding, B. *Chem. Soc. Rev.* **1996**, *25*, 329.
- Reitzer, R.; Gruber, K.; Jogl, G.; Wagner, U. G.; Bothe, H.; Buckel, W.; Kratky, C. *Structure* **1999**, *7*, 891.
- (a) Mancía, F.; Keep, N. H.; Nakagawa, A.; Leadlay, P. F.; McSweeney, S.; Rasmussen, B.; Bosecke, P.; Diat, O.; Evans, P. R. *Structure* **1996**, *4*, 339. (b) Mancía, F.; Evans, P. R. *Structure* **1998**, *6*, 711.
- (a) Moore, B. S.; Eisenberg, R.; Weber, C.; Bridges, A.; Nanz, D.; Robinson, J. A. *J. Am. Chem. Soc.* **1995**, *117*, 11285. (b) Zerber-Burkhardt, K.; Ratnatilleke, A.; Phillipon, N.; Birch, A.; Leiser, A.; Vrijbloed, J. W. *J. Biol. Chem.* **1998**, *273*, 6508.
- (a) Abeles, R. H.; Dolphin, D. *Acc. Chem. Res.* **1976**, *9*, 114. (b) Toraya, T. Diol dehydratase and glycerol dehydratase. In *Chemistry and Biochemistry of B<sub>12</sub>*; Banerjee, R., Ed.; Wiley: New York, 1999; pp 783–809.
- Toraya, T.; Fukui, S. *Eur. J. Biochem.* **1977**, *76*, 285.
- (a) Babior, B. M. *J. Biol. Chem.* **1970**, *245*, 6125. (b) Trommel, J. S.; Warncke, K.; Marzilli, L. G. *J. Am. Chem. Soc.* **2001**, *123*, 3358. (c) Warncke, K.; Utada, A. S. *J. Am. Chem. Soc.* **2001**, *123*, 8564. (d) Ke, S.-C.; Torrent, M.; Museav, D. G.; Morokuma, K.; Warncke, K. *Biochemistry* **1999**, *38*, 12681. (e) Warncke, K.; Schmidt, J. C.; Ke, S.-C. *J. Am. Chem. Soc.* **1999**, *121*, 10522. (f) Ke, S.-C.; Warncke, K. *J. Am. Chem. Soc.* **1999**, *121*, 9922.
- (a) Stadtman, T. C. *Adv. Enzymol.* **1973**, *38*, 413. (b) Tang, K.-H.; Chang, C. H.; Frey, P. A. *Biochemistry* **2001**, *40*, 5190. (c) Chang, C. H.; Frey, P. A. *J. Biol. Chem.* **2000**, *275*, 106.
- (a) Kunz, F.; Rétey, J.; Arigoni, D.; Tsai, L.; Stadtman, T. C. *Helv. Chim. Acta* **1978**, *61*, 1139. (b) Rétey, J.; Kunz, F.; Arigoni, D.; Stadtman, T. C. *Helv. Chim. Acta* **1978**, *61*, 2989.
- Chen, H.-P.; Wu, S.-H.; Lin, Y.-L.; Chen, C.-H.; Tsay, S.-I. *J. Biol. Chem.* **2001**, *276*, 44744.
- Bevan, W. I.; Haszeldine, R. N.; Middleton, J.; Tipping, A. E. *J. Organomet. Chem.* **1973**, *47*, 53.
- Brook, A. G.; Jones, P. F. *Chem. Comm.* **1969**, 1324.
- Bürger, H.; Moritz, P. *Organometallics* **1993**, *12*, 4930.
- Reetz, M. T.; Greif, N. *Angew. Chem., Int. Ed. Engl.* **1977**, *16*, 712.
- Sakurai, H.; Hosomi, A.; Kumada, M. *Chem. Comm.* **1969**, 451.
- Claes, L.; François, J.-P.; Deleuze, M. S. *J. Am. Chem. Soc.* **2003**, *125*, 7129.
- Naka, A.; Ueda, S.; Ohshita, J.; Kunai, A.; Miura, T.; Kobayashi, H.; Ishikawa, M. *Organometallics* **2008**, *27*, 2922.
- Yu, Y.; Feng, S.; Feng, D. *J. Phys. Chem. A* **2005**, *109*, 3663.
- Yu, Y.; Feng, S. *J. Phys. Chem. A* **2006**, *110*, 12463.
- Yu, Y.; Feng, S. *Int. J. Quantum Chem.* **2007**, *107*, 105.
- Brook, A. G. *Acc. Chem. Res.* **1974**, *7*, 77.
- Martin, J. G.; Ring, M. A.; O'Neal, H. E. *Organometallics* **1986**, *5*, 1228.
- Bakhtiar, R.; Holznagel, C. M.; Jacobson, D. B. *Organometallics* **1993**, *12*, 621.
- Willard, B. B.; Graul, S. T. *J. Phys. Chem. A* **1998**, *102*, 6942.
- Holtmann, U.; Jutzi, P.; Kühler, T.; Neumann, B.; Stammer, H.-G. *Organometallics* **1999**, *18*, 5531.
- (a) Yokelson, H. B.; Maxka, J.; Siegel, D. A.; West, R. *J. Am. Chem. Soc.* **1986**, *108*, 4239. (b) Yokelson, H. B.; Siegel, D. A.; Millevolte, A. J.; Maxka, J.; West, R. *Organometallics* **1990**, *9*, 1005.
- Iwamoto, T.; Okita, J.; Kabuto, C.; Kira, M. *J. Organomet. Chem.* **2003**, *686*, 105.
- Sekiguchi, A.; Izumi, R.; Lee, V. Y.; Ichinohe, M. *Organometallics* **2003**, *22*, 1483.
- (a) Reetz, M. T.; Kliment, M.; Plachky, M. *Angew. Chem., Int. Ed. Engl.* **1974**, *13*, 813. (b) Reetz, M. T.; Kliment, M.; Plachky, M. *Chem. Ber.* **1976**, *108*, 2716. (c) Reetz, M. T.; Kliment, M.; Plachky, M.; Greif, N. *Chem. Ber.* **1976**, *108*, 2728.
- Schwartz, H.; Wesdemiotis, C.; Reetz, M. T. *J. Organomet. Chem.* **1978**, *161*, 153.
- Reetz, M. T.; Kliment, M. *Tetrahedron Lett.* **1975**, 2909.
- Haas, A. *Angew. Chem., Int. Ed. Engl.* **1965**, *4*, 1014.
- Schöllkopf, U. *Angew. Chem., Int. Ed. Engl.* **1970**, *9*, 763.
- Lithium complexation appears to be involved in the aza-Wittig rearrangement. See: Reetz, M. T.; Schinzer, D. *Tetrahedron Lett.* **1975**, 3485.
- Davies, J. W.; Malpass, J. R.; Walker, M. P. *Chem. Comm.* **1985**, 686.
- Frainnet, E.; Duboudin, F.; Debescat, F.; Vincon, G. *C. R. Acad. Sci., Ser. C* **1973**, *276*, 1469.
- (a) Nowakowski, P.; West, R. *J. Am. Chem. Soc.* **1976**, *98*, 5616. (b) West, R.; Nowakowski, P.; Boudjouk, P. *J. Am. Chem. Soc.* **1976**, *98*, 5620.
- (a) Wolfgramm, R.; Klingebiel, U. *Z. Anorg. Allg. Chem.* **1998**, *624*, 1031. (b) Wolfgramm, R.; Müller, T.; Klingebiel, U. *Organometallics* **1998**, *17*, 3222.
- Diedrich, F.; Klingebiel, U.; Schäfer, M. *J. Organomet. Chem.* **1999**, *588*, 242.
- Ebker, C.; Schmatz, S.; Diedrich, F.; Klingebiel, U. *Silicon Chem.* **2003**, *2*, 117.



- (74) Albrecht, T.; Elter, G.; Meller, A. *Z. Anorg. Allg. Chem.* **1999**, *625*, 1453.
- (75) Wannagat, U. *Organomet. Chem. IUPAC Symp.* **1966**, *1*, 274.
- (76) Gellermann, E.; Klingebiel, U.; Pape, T.; Dall'Antonia, F.; Schneider, T. R.; Schmatz, S. *Z. Anorg. Allg. Chem.* **2001**, *627*, 2581.
- (77) Aumann, R. *Angew. Chem., Int. Ed. Engl.* **1971**, *10*, 189.
- (78) Wayland, B. B.; Feng, Y.; Ba, S. *Organometallics* **1989**, *8*, 1438.
- (79) Breimair, J.; Niemer, B.; Raab, K.; Beck, W. *Chem. Ber.* **1991**, *124*, 1059.
- (80) Chu, K.-H.; Foxman, B. M.; Rosenblum, M.; Zhu, X.-Y. *Organometallics* **1990**, *9*, 3010.
- (81) Wheatley, B. M. M.; Keay, B. A. *J. Org. Chem.* **2007**, *72*, 7253.
- (82) (a) Erker, G.; Kropp, K. *Chem. Ber.* **1982**, *115*, 2437. (b) Erker, G.; Kropp, K.; Krfiger, C.; Chiang, A.-P. *Chem. Ber.* **1982**, *115*, 2447.
- (83) Erker, G. *Acc. Chem. Res.* **1984**, *17*, 103.
- (84) (a) Erker, G.; Rosenfeldt, F. *J. Organomet. Chem.* **1980**, *188*, C1. (b) Erker, G.; Rosenfeldt, F. *Angew. Chem., Int. Ed. Engl.* **1978**, *17*, 605.
- (85) Erker, G.; Dorf, U.; Czisch, P.; Petersen, J. L. *Organometallics* **1986**, *5*, 668.
- (86) Curtis, C. J.; Haltiwanger, R. C. *Organometallics* **1991**, *20*, 3220.
- (87) Erker, G.; Bendix, M.; Petrenz, R. *Organometallics* **1992**, *11*, 1646.
- (88) Ward, A. S.; Mintz, E. A.; Kramer, M. P. *Organometallics* **1988**, *7*, 8.
- (89) Erker, G.; Petrenz, R. *Chem. Comm.* **1989**, 345.
- (90) Erker, G.; Petrenz, R. *Organometallics* **1992**, *11*, 1646.
- (91) (a) Braunstein, P.; Knorr, M.; Hirle, B.; Reinhard, G.; Schubert, U. *Angew. Chem., Int. Ed. Engl.* **1992**, *104*, 1583. (b) Braunstein, P.; Knorr, M.; Reinhard, G.; Schubert, U.; Stährfeldt, T. *Chem.—Eur. J.* **2000**, *6*, 4265.
- (92) Messaoudi, A.; Deglmann, P.; Braunstein, P.; Hofmann, P. *Inorg. Chem.* **2007**, *46*, 7899.
- (93) Steinmetz, M. G.; Langston, M. A.; Mayes, R. T.; Udayakumar, B. S. *J. Org. Chem.* **1986**, *51*, 5051.
- (94) Baines, K. M.; Brook, A. G.; Ford, R. R.; Lickiss, P. D.; Saxena, A. K.; Chatterton, W. J.; Sawyer, J. F.; Behnam, B. A. *Organometallics* **1989**, *8*, 693.
- (95) Sierra, M. A.; Fernández, I.; Mancheño, M. J.; Gómez-Gallego, M.; Torres, M. R.; Cossío, F. P.; Arrieta, A.; Lecea, B.; Poveda, A.; Jiménez-Barbero, J. *J. Am. Chem. Soc.* **2003**, *125*, 9572.
- (96) Fernández, I.; Sierra, M. A.; Gómez-Gallego, M.; Mancheño, M. J.; Cossío, F. P. *Angew. Chem., Int. Ed.* **2006**, *45*, 125.
- (97) Fernández, I.; Sierra, M. A.; Gómez-Gallego, M.; Mancheño, M. J.; Cossío, F. P. *Eur. J. Inorg. Chem.* **2008**, 2454.
- (98) Woodward, R. B.; Hoffmann, R. *Angew. Chem.* **1969**, *81*, 797; *Angew. Chem., Int. Ed.* **1969**, *8*, 781.
- (99) (a) Mackenzie, K. *J. Chem. Soc.* **1965**, 4646. (b) Mackenzie, K. *J. Chem. Soc.* **1965**, 4650.
- (100) (a) Mackenzie, K. *J. Chem. Soc. C* **1969**, 480. (b) Mackenzie, K. *J. Chem. Soc. C* **1969**, 1784.
- (101) Wilson, C.; Howard, J. A. K. *Acta Crystallogr.* **1998**, *C54*, 544.
- (102) (a) Mackenzie, K.; Proctor, G.; Woodnut, D. J. *Tetrahedron Lett.* **1984**, *25*, 977. (b) Howard, J. A. K.; Mackenzie, K.; Johnson, R. E. *Tetrahedron Lett.* **1989**, *30*, 5005.
- (103) Mackenzie, K.; Proctor, G.; Woodnut, D. J. *Tetrahedron* **1987**, *43*, 5981.
- (104) Chow, T. S. *J. Chin. Chem. Soc.* **1996**, *43*, 101.
- (105) Mackenzie, K.; Howard, J. A. K.; Mason, S.; Gravett, E. C.; Astin, K. B.; Liu, S. X.; Batsanov, A. S.; Vlaovic, D.; Maher, J. P. *J. Chem. Soc., Perkin Trans. 2* **1993**, *6*, 1211.
- (106) Mackenzie, K.; Howard, J. A. K.; Siedlecka, R.; Astin, K. B.; Gravett, E. C.; Wilson, C.; Cole, J.; Gregory, R. G.; Tomlins, A. S. *J. Chem. Soc., Perkin Trans. 2* **1996**, *8*, 1749.
- (107) (a) Mackenzie, K.; Gravett, E. C.; Gregory, R. J.; Howard, J. A. K.; Maher, J. P. *Tetrahedron Lett.* **1992**, *33*, 5629. (b) Mackenzie, K.; Astin, K. B.; Gravett, E. C.; Gregory, R. J.; Howard, J. A. K.; Wilson, C. *J. Phys. Org. Chem.* **1998**, *11*, 879.
- (108) Mackenzie, K. *Recent Dev. Org. Chem.* **2000**, *4*, 295.
- (109) Hagenbuch, J.-P.; Stampfli, B.; Vogel, P. *J. Am. Chem. Soc.* **1981**, *103*, 3934.
- (110) Paquette, L. A.; Kesselmayer, M. A.; Rogers, R. D. *J. Am. Chem. Soc.* **1990**, *112*, 284.
- (111) Paquette, L. A.; O'Doherty, G. A.; Rogers, R. D. *J. Am. Chem. Soc.* **1991**, *113*, 7761.
- (112) O'Doherty, G. A.; Rogers, R. D.; Paquette, L. A. *J. Am. Chem. Soc.* **1994**, *116*, 10883.
- (113) Houk, K. N.; Li, J. Y.; McAllister, M. A.; O'Doherty, G. A.; Paquette, L. A.; Siebrand, W.; Smedarchinal, Z. K. *J. Am. Chem. Soc.* **1994**, *116*, 10895.
- (114) Grimme, W.; Pohl, K.; Wortmann, J.; Frowein, D. *Liebigs Ann.* **1996**, *11*, 1905.
- (115) Becka, K.; Branda, U.; Hünig, S.; Martin, H.-D.; Mayer, B.; Peters, K.; von Schnering, H. G. *Liebigs Ann.* **1996**, *11*, 1881.
- (116) Chow, T. J.; Ding, M.-F. *Angew. Chem., Int. Ed. Engl.* **1986**, *25*, 1121.
- (117) Marchand, A. P.; Annapurna, P.; Watson, W. H.; Nagl, A. *Chem. Comm.* **1989**, 281.
- (118) Geich, H.; Grimme, W.; Proske, K. *J. Am. Chem. Soc.* **1992**, *114*, 1492.
- (119) (a) Herzschuh, R.; Rabbih, R. M.; Kühn, H.; Mühlstädt, M. *Int. J. Mass Spectrom. Ion Phys.* **1983**, *47*, 387. (b) Klufft, E.; Nibbering, N. M. M.; Kühn, H.; Herzschuh, R. *J. Am. Chem. Soc.* **1986**, *108*, 7201.
- (120) Nibbering, N. M. M.; van der Hart, W. J. *J. Am. Soc. Mass Spectrom.* **2002**, *13*, 1186.
- (121) Edelman, M. A.; Hitchcock, P. B.; Lappert, M. F.; Liu, D.-S.; Tian, S. *J. Organomet. Chem.* **1998**, *550*, 397.
- (122) Singh, G.; Linden, A.; Abou-Hadeed, K.; Hansen, H.-J. *Helv. Chim. Acta* **2002**, *85*, 27.
- (123) Lin, S.; Danishefsky, S. J. *Angew. Chem., Int. Ed.* **2002**, *41*, 512, and references therein.
- (124) Goldschmidt, Z.; Antebi, S. *Tetrahedron Lett.* **1978**, *3*, 271.
- (125) Collum, D. B.; Klang, J. A.; Depue, R. T. *J. Am. Chem. Soc.* **1986**, *108*, 2333.
- (126) Wolffe, I.; Chan, S.; Schuster, G. B. *J. Org. Chem.* **1991**, *56*, 7313.
- (127) Stone, A.; Wales, D. J. *Chem. Phys. Lett.* **1986**, *128*, 501.
- (128) Jin, Y.-F.; Hao, C. *J. Phys. Chem. A* **2005**, *109*, 2875.
- (129) (a) Murry, R. L.; Strout, D. L.; Odum, G. K.; Scuseria, G. E. *Nature* **1993**, *366*, 665. (b) Yi, J.-Y.; Bernhole, J. *J. Chem. Phys.* **1992**, *96*, 8634.
- (130) Honda, K.; Osawa, E. *Fullerene Sci. Technol.* **1996**, *4*, 925.
- (131) Bettinger, H. F.; Jakobson, B. I.; Scuseria, G. E. *J. Am. Chem. Soc.* **2003**, *125*, 5572.
- (132) Choi, W. I.; Kim, G.; Han, S.; Ihm, J. *Phys. Rev. B* **2006**, *73*, 113406.
- (133) Buchanan, J. G.; Ruggiero, G.; Williams, I. H. *Org. Biomol. Chem.* **2008**, *6*, 66.
- (134) Gutta, P.; Tantillo, D. J. *J. Am. Chem. Soc.* **2006**, *128*, 6172.
- (135) Yu, Y.; Feng, S.; Feng, D. *J. Phys. Chem. A* **2005**, *109*, 3663.
- (136) Yu, Y.; Feng, S. *J. Phys. Chem. A* **2006**, *110*, 12463.
- (137) Yu, Y.; Feng, S. *Int. J. Quantum Chem.* **2007**, *107*, 105.
- (138) (a) Miller, W. W.; Richards, J. H. *J. Am. Chem. Soc.* **1969**, *91*, 1498. (b) Choi, G.; Choi, S.-C.; Galan, A.; Wilk, B.; Dowd, P. *Proc. Natl. Acad. Sci. U.S.A.* **1990**, *87*, 3174. (c) Pratt, J. M. *Chem. Soc. Rev.* **1985**, *14*, 161.
- (139) (a) Dixon, R. M.; Golding, B. T.; Mwesigye-Kibende, S.; Rao, D. N. R. *Philos. Trans. R. Soc. Lond.* **1985**, *B311*, 531. (b) Dong, S.; Padmakumar, R.; Banerjee, R.; Spiro, T. G. *J. Am. Chem. Soc.* **1999**, *121*, 7063. (c) Gruber, K.; Reitzer, R.; Kratky, C. *Angew. Chem., Int. Ed.* **2001**, *40*, 3377. (d) Tang, K.-H.; Harms, A.; Frey, P. A. *Biochemistry* **2002**, *41*, 8767. (e) Brooks, A. J.; Vlaisse, M.; Banerjee, R.; Brunold, T. C. *J. Am. Chem. Soc.* **2005**, *127*, 16522. (f) Buckel, W.; Pierik, A. J.; Plett, S.; Alhappel, S.; Suarez, D.; Tu, S.-M.; Golding, B. T. *Eur. J. Inorg. Chem.* **2006**, 3622.
- (140) (a) Semialjac, M.; Schwartz, H. *J. Am. Chem. Soc.* **2002**, *124*, 8974. (b) Khoroshun, D. V.; Warncke, K.; Ke, S.-C.; Musaev, D. G.; Morokuma, K. *J. Am. Chem. Soc.* **2003**, *125*, 570. (c) Brooks, A. J.; Vlaisse, M.; Banerjee, R.; Brunold, T. C. *J. Am. Chem. Soc.* **2004**, *126*, 8167. (d) Kozlowski, P. M. *Curr. Opin. Chem. Biol.* **2001**, *5*, 736. (e) Kozlowski, P. M.; Kamachi, T.; Toraya, T.; Yoshizawa, K. *Angew. Chem., Int. Ed.* **2007**, *46*, 980.
- (141) Smith, D. M.; Golding, B. T.; Radom, L. *J. Am. Chem. Soc.* **1999**, *121*, 9388.
- (142) (a) Smith, D. M.; Golding, B. T.; Radom, L. *J. Am. Chem. Soc.* **2001**, *123*, 1664. (b) Kinoshita, K.; Kawata, M.; Ogura, K.-i.; Yamasaki, A.; Watanabe, T.; Komoto, N.; Hieda, N.; Yamanishi, M.; Tobimatsu, T. *Biochemistry* **2008**, *47*, 3162. (c) Kamachi, T.; Toraya, T.; Yoshizawa, K. *Chem.—Eur. J.* **2007**, *13*, 7864.
- (143) (a) Sandala, G. M.; Smith, D. M.; Radom, L. *J. Am. Chem. Soc.* **2006**, *128*, 16004. (b) Wetmore, S. D.; Smith, D. M.; Radom, L. *J. Am. Chem. Soc.* **2001**, *123*, 8678.
- (144) (a) Reetz, M. T.; Neumeier, G. *Liebigs Ann. Chem.* **1981**, 1234. (b) Reetz, M. T.; Neumeier, G.; Kaschube, M. *Tetrahedron Lett.* **1975**, 1295.
- (145) Fernández, I.; Sierra, M. A.; Cossío, F. P. *J. Org. Chem.* **2007**, *72*, 1488.
- (146) Frenking, G.; Cossío, F. P.; Sierra, M. A.; Fernández, I. *Eur. J. Org. Chem.* **2007**, 5410.
- (147) Fernández, I.; Frenking, G. *Faraday Discuss.* **2007**, *135*, 403.
- (148) Deng, Q.; Thomas, B. E., IV; Houk, K. N.; Dowd, P. *J. Am. Chem. Soc.* **1997**, *119*, 6902.
- (149) Zhang, X.; Houk, K. N.; Lin, S.; Danishefsky, S. J. *J. Am. Chem. Soc.* **2003**, *125*, 5111.
- (150) Barton, T. J.; Groh, B. L. *J. Am. Chem. Soc.* **1985**, *107*, 7221.
- (151) Komatsu, M.; Okada, H.; Akaki, T.; Oderaotoshi, Y.; Minakata, S. *Org. Lett.* **2002**, *4*, 3505.



- (152) Li, W.; LaCour, T. G.; Fuchs, P. L. *J. Am. Chem. Soc.* **2002**, *124*, 4548.
- (153) For apparent examples of 6- to 5-ring lactone dyotropic rearrangements, see: (a) Evans, R. H., Jr.; Ellestad, G. A.; Kunstmann, M. P. *Tetrahedron Lett.* **1969**, 1791. and. (b) Cambie, R. C.; McNally, H. M.; Robertson, J. D.; Rutledge, P. S.; Woodgate, P. D. *Aust. J. Chem.* **1984**, *37*, 409 For 5- to 6-ring lactone rearrangement. (c) Marson, C. M.; Grabowska, U.; Walsgrove, T.; Eggleston, D. S.; Baures, P. W. *J. Org. Chem.* **1994**, *59*, 284.
- (154) Fujisawa, T.; Kurita, Y.; Kawashima, M.; Sato, T. *Chem. Lett.* **1982**, 1641.
- (155) Kocienski, P.; Wadman, S. *J. Am. Chem. Soc.* **1989**, *111*, 2362.
- (156) Kocienski, P.; Barber, C. *Pure Appl. Chem.* **1990**, *62*, 1933, and references therein.
- (157) Takle, A.; Kocienski, P. *Tetrahedron* **1990**, *46*, 4503.
- (158) Stocks, M.; Kocienski, P.; Donald, D. K. *Tetrahedron Lett.* **1990**, *31*, 1637.
- (159) (a) Kocienski, P.; Yeates, C.; Street, S. D. A.; Campbell, S. F. *J. Chem. Soc., Perkin Trans.* **1987**, 2183. (b) Kocienski, P.; Street, S. D. A.; Yeates, C.; Campbell, S. F. *J. Chem. Soc., Perkin Trans.* **1987**, 2189.
- (160) Kocienski, P.; Love, C. J.; Whitby, R. J.; Costello, G.; Roberts, D. A. *Tetrahedron* **1989**, *45*, 3839.
- (161) Lemos, E.; Porée, F.-H.; Commerçon, A.; Betzer, J.-F.; Pancrazi, A.; Ardisson, J. *Angew. Chem., Int. Ed.* **2007**, *46*, 1917.
- (162) For related examples from the same group, see: (a) Le Ménez, P.; Fargeas, V.; Berque, I.; Poisson, J.; Ardisson, J.; Lallemand, J.-Y.; Pancrazi, A. *J. Org. Chem.* **1995**, *60*, 3592. (b) Fargeas, V.; Le Ménez, P.; Berque, I.; Ardisson, J.; Pancrazi, A. *Tetrahedron* **1996**, *52*, 6613.
- (163) Zweifel, G.; Arzoumanian, H. *J. Am. Chem. Soc.* **1967**, *89*, 5086.
- (164) Harada, T.; Hara, D.; Hattori, K.; Oku, A. *Tetrahedron Lett.* **1988**, *29*, 3821.
- (165) Negishi, E.; Akiyoshi, K.; OConnor, B.; Takagi, K.; Wu, G. *J. Am. Chem. Soc.* **1989**, *111*, 3089.
- (166) Alexakis, A.; Hanaizi, J.; Jachiet, D.; Normant, J.-F.; Toupet, L. *Tetrahedron Lett.* **1990**, *31*, 1271.
- (167) Denmark, S. E.; Montgomery, J. I. *Angew. Chem., Int. Ed.* **2005**, *44*, 3732.
- (168) Denmark, S. E.; Montgomery, J. I.; Kramps, L. A. *J. Am. Chem. Soc.* **2006**, *128*, 11620.

CR900209C